

DTIC FILE COPY

2

Naval Ocean Research and Development Activity

February 1989

Report 199



AD-A208 597

**Geologic Study of Five Sites in the
Western North Atlantic Ocean**

DTIC
ELECTE
JUN 05 1989
S D

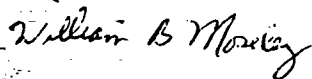
Muriel S. Grim
Frederick A. Bowles
Joseph F. Gettrust
Don A. Burns
Seafloor Geosciences Division
Ocean Science Directorate

89 6 05 034


Foreword

Acoustic signals in the ocean interact with the water/sediment boundary and travel along subbottom paths. Navy scientists have always been concerned about the effect of the geologic environment on the acoustic signals. For programs that study bottom interaction of very-low-frequency acoustic signals to be effective, a complete and accurate picture of the geology along the travel path is required.

In this report the geology of five areas of the western North Atlantic Ocean is described. The similarities and differences among the sites are noted. Two sites are examined in detail. Geoacoustic models, which take into account the geologic conditions peculiar to these sites, are presented.



W. B. Moseley
Technical Director



A. C. Esau, Captain, USN
Commanding Officer

Executive Summary

For an accurate geoacoustic model to be constructed, the geology of the area must be well understood. In some areas modeling may not be successful because small-scale lithologic and topographic changes are not recognized from the available data. Currently, we do not have the ability to obtain complete measurements of such sediment properties as velocity and density from a drill hole. Laboratory and in situ measurements do not agree, and attempts to reconcile the two have not been completely effective. In constructing our geoacoustic models we have tried to build on the work of others. In our models, we have added high-velocity stringers which are almost always present in nature; for example, worldwide occurrences of chert have been documented by Deep-Sea Drilling Project (DSDP) cores.

We chose five areas of the western North Atlantic Ocean and constructed geoacoustic models for each area. For two areas we used the laboratory and seismic data collected during DSDP studies, as well as published reports, to construct detailed models. For the remaining three areas we have tabulated generalized sediment velocity and lithology information from published reports.

In working on data from these five sites it became apparent to us that some areas (for example, the Bahama Banks) have such rugged topography and such variable lithology that traditional modeling attempts probably will be unsuccessful unless the geology is known in great detail. Some continental margin shallow-water sites and some deep ocean sites, such as DSDP site 417/418, are much more predictable and should be easier to model; however, even site 417/418 has unique geologic factors that will cause actual seismic propagation to differ from our model predictions. However, deviations from predicted values should be reasonably small at low (5-50 Hz) frequencies.



Accession For	
NTIS CR&I	<input checked="" type="checkbox"/>
DTIC TAB	<input type="checkbox"/>
Unannounced	<input checked="" type="checkbox"/>
Justification	
By	
Distribution	
Availability Codes	
Dist	Avail and/or Special
A-1	

Acknowledgments

We thank J. A. Ballard for reviewing the manuscript. We acknowledge helpful discussions with R. Bennett, J. Egloff, C. Sellinger, and D. Lavoie, whose assistance in assembling some of the information contained in this report is also appreciated.

This work was funded by the Office of Naval Technology under Program Element 62435N, H. C. Eppert, Jr., program manager.

Contents

I. Introduction	1
II. Area I: Blake-Bahama Basin (DSDP Hole 534)	1
A. Geologic Setting	1
B. Seismic Stratigraphy	5
C. Geologic Factors Impacting Seismic Propagation	6
D. Velocity and Density Profiles	8
III. Area II: Nares Abyssal Plain (DSDP Holes 417/418)	8
A. Geologic Setting	8
B. Seismic Stratigraphy	9
C. Oblique Seismic Experiment	10
D. Geologic Factors Impacting Seismic Propagation	10
E. Velocity and Density Profiles	10
IV. Area III: Blake Plateau	11
A. Geologic Setting	11
B. Geologic Factors Impacting Seismic Propagation	13
V. Area IV: Bahama Platform	14
A. Geologic Setting	14
B. Geologic Factors Affecting Seismic Propagation	14
VI. Area V: The Bermuda Rise	14
A. Geologic Setting	14
B. Seismic Stratigraphy	15
C. Geologic Factors Affecting Seismic Propagation	16
VII. Bottom Current Descriptions for 82°W-65°W, 23°N-33°N	16
A. Previous OBS Efforts	16
B. General Deep Circulation	16
C. Circulation Variability	17
D. Best Estimate of Subsurface Currents	17
E. Conclusions	17
VIII. Geoacoustic Models	19
A. Area I: Seismic Models	19
B. Area II: Seismic Model	22
C. Area III: Seismic Model	24
D. Area IV: Velocity Profiles	24
E. Area V: Seismic Model	24

IX. Summary and Conclusions	24
X. References	26
Appendix A-1	
Listing of Laboratory-measured Physical Properties for Sediments from DSDP Sites 534 and 391	29
Appendix A-2	
Listing of Laboratory-measured Physical Properties for Sediments from DSDP Holes 417 and 418	39
Appendix A-3	
Listing of Laboratory-measured Physical Properties for Sediments from DSDP Site 386	47
Appendix A-4	
Plot of Laboratory-measured Velocity as a Function of Depth for Cores from Hole 386	51

Geologic Study of Five Sites in the Western North Atlantic Ocean

I. Introduction

Simple, layered models are rarely adequate descriptions of the earth's structure, particularly over large distances. We must be cognizant of geologic features that might substantially alter acoustic wave propagation. In this report, geologic descriptions and a summary of pertinent information from Deep Sea Drilling Project (DSDP) site reports are presented with geoacoustic models so that the impact of this information can be considered when building models to predict acoustic wave propagation.

Geoacoustic model parameters for five sites in the Northwest Atlantic were derived from DSDP and other published studies. The measurements of physical properties made on samples from drill holes provide both qualitative and quantitative information; several factors degrade the latter. For geoacoustic purposes, the most important factors are (1) the percentage of cored section recovered for the uppermost sediments is usually less than 50%; (2) the laboratory measurements do not duplicate the pressure and temperature environment from which the sediments came; and (3) the samples are smaller than many features (e.g., cracks and fissures) that affect seismic properties. Nonetheless, the data from the drill holes provide the only definite identification of the sediments and their geoacoustic properties. In constructing the geoacoustic models, attempts were made to adjust the laboratory measurements to in situ values and to correct or eliminate obviously erroneous data.

Hamilton's modeling work (1980) provides most of the empirically derived relationships used in preparing these geoacoustic models. A study made near DSDP site 417 by Tucholke and Shirley (1979) provides insight into the differences between laboratory and in situ velocity measurements in the uppermost few meters of sediment. Milholland et al. (1980) studied the relationship between physical and acoustic properties of deep-sea carbonate sediments in the southwestern Pacific. They examined variations in density, velocity, and anisotropy as functions of depth, diagenetic stage, and clay enrichment. Christensen and Salisbury (1975) studied the differences between in situ and laboratory-measured velocities for basalts. The work of these investigators, as well as that of Nafe and Drake (1963)

and Ludwig et al. (1970), were used where the velocity-density-depth information from the site did not fit the Hamilton curves.

In the following sections, we describe the geologic setting for five sites, the seismic (geoacoustic) information available about the sediments and upper oceanic crust, and the geoacoustic implications that can be drawn from this information. Because deep ocean currents can affect the methods used to emplace bottom sensors and the ambient noise level, bottom currents are discussed.

II. Area I: Blake-Bahama Basin (DSDP Hole 534)

A. Geologic Setting

The Blake-Bahama Basin lies off the southeastern coast of the United States in 4800 to 5000 m of water. It is surrounded by the Blake Escarpment to the west, the Bahama Escarpment to the south, and the Blake-Bahama Outer Ridge to the east and north (Fig. 1). The central part of the basin has been extensively surveyed using single and multichannel seismic reflection methods (Fig. 2). Prior to 1975 most of the data from this area were collected by the Lamont-Doherty Geological Observatory. More recently, multichannel data were collected by other academic institutions and the U.S. Geological Survey. Table 1 lists the names and dates of cruises on which multichannel data were collected in the immediate vicinity of DSDP site 534.

Site 534 is located in the Blake-Bahama Basin about 100 km east of the base of the Blake Escarpment and approximately the same distance west of the Blake-Bahama Outer Ridge. The site is approximately 22 km northeast of DSDP site 391. Detailed bathymetry of

Table 1. Information on multichannel tracklines in Blake-Bahama Basin.

AGENCY	DATE	CRUISE	LINE NUMBERS
LDGO	1977	RC-2102	MC88, MC89, MC90, MC95, MC96
LDGO	1975	RC-1903	MC1
USGS	1978	TD	TD-2, TD-3, TD-4
USGS	1975	FC	FC-1, FC-2, FC-3

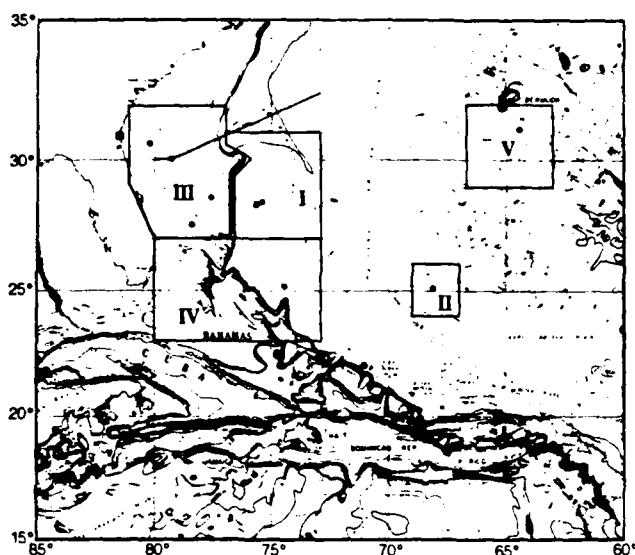


Figure 1. Location map for the areas discussed in the report. Dots indicate the locations of DSDP drill sites. Physiographic provinces are labeled. The location of a cross section (Fig. 6) through the Blake Plateau and the Blake Outer Ridge is indicated by the line that crosses these features.

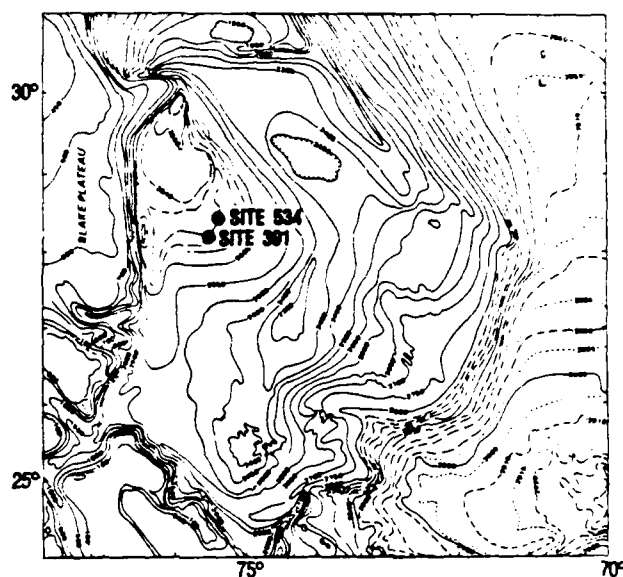


Figure 3. Detailed bathymetry of the Blake-Bahama Basin (adapted from the Initial Reports of the DSDP, v. 44, 1978). Depths are in fathoms. Locations of sites 534 and 391 are indicated.

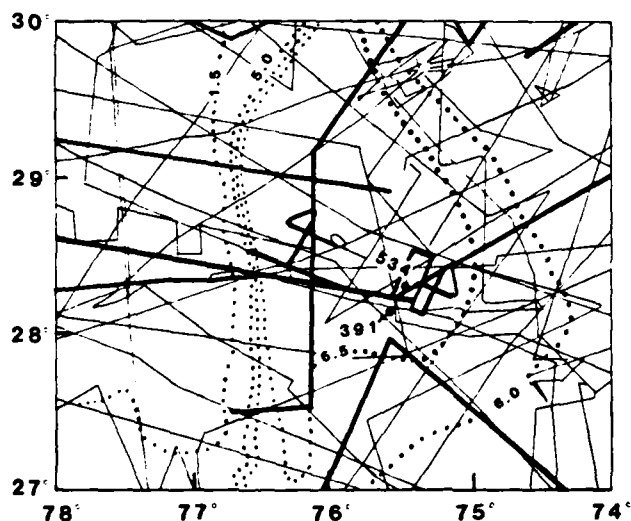


Figure 2. Track lines of single-channel (thin lines) and multichannel (thick lines) seismic reflection surveys in the Blake-Bahama Basin and Blake Outer Ridge area. Dotted lines are bathymetric contours in seconds (two-way travel time). After Markl and Bryan, 1983.

the basin and locations of sites 534 and 391 are shown in Figure 3.

The basement, composed of oceanic basalts, is buried beneath 1600 to 2000 m of sediment. Basement relief in the vicinity of the drill site is about 400 m (0.2 to 0.04 sec two-way travel time) as shown in Figure 4.

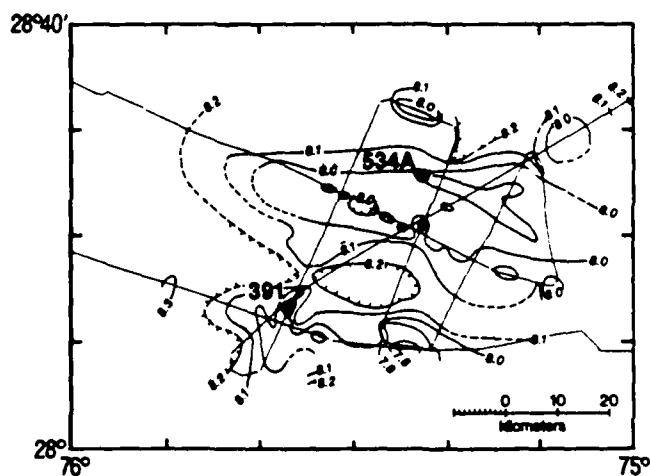


Figure 4. Contour map of the basement in the vicinity of DSDP sites 391 and 534. Contours (modified from Bryan et al., 1980) are in seconds of two-way travel time. Dotted lines show bathymetry trackline locations used in making the contour map.

Hole 534 was drilled at a basement high because the primary objective of the survey was to reach basement and obtain samples of the oldest Atlantic Ocean sediments. In hole 534A basement was reached at 1635 m below the sea floor. The shipboard party decided that the upper sedimentary column was similar

enough to that of hole 391 that coring and logging were not begun until the hole had been drilled to a depth of 545 m.

Various seismic reflectors observed on the reflection data have been identified and correlated with reflectors recognized throughout the western North American Basin. From uppermost to lowest in the sediment column, the reflectors have been labeled M, X series, A series, b', b, C', C, D', D, and basement (Table 2). By tracing these reflectors to outcrops and DSDP drill holes and by incorporating information from many geophysical and geological studies, researchers have deduced the following geologic history of the area.

The Blake-Bahama Basin contains some of the oldest basement rock in the North Atlantic Ocean. The Blake Spur Magnetic Anomaly (BSMA) crosses the basin from northeast to southwest (Fig. 5). Seaward of the BSMA are the low-amplitude anomalies of the Jurassic Magnetic Quiet Zone. Anomaly M-28, proposed by Bryan et al. (1980) on the basis of scant data, would be the oldest in this group.

Oceanic crust associated with anomaly M-28 was sampled at DSDP drill site 534. The penecontemporaneous sediments lying above the basalts were identified as Callovian (mid-Jurassic) in age, which is equivalent to approximately 165 million years (Childs, 1985).

Oceanic crust between the BSMA and the east coast Magnetic Anomaly (located along the continental margin at the continental-oceanic crust boundary) is thought to be a remnant of the initial opening phase of the Mesozoic Atlantic (Vogt, 1973; Sheridan, 1978; Klitgord and Behrendt, 1979). These authors suggest that this crust was formed at an extinct spreading center, which later shifted to location at the BSMA. As a result, the crust was isolated and became a part of the North American margin.

In addition to the change in magnetic signature observed across the BSMA, there is also a structural change in the basement. Shoreward of the BSMA the basement is deeper and rougher than it is on the seaward side (Grow and Markl, 1977; Shipley et al., 1978). At the approximate location of the BSMA,

Table 2. Geologic formations of the Blake-Bahama Basin.

FORMATION	AGE	LITHOLOGY	SEISMIC EVENTS
Blake Ridge	Present to mid-Eocene	ooze, silt, silty clay, chalk, mudstone, turbidites	M
			X
Bermuda Rise	mid-Eocene to Late Paleocene	ooze, clay chert	A ^u , A ^c
Plantagenet	Late Paleocene to Cenomanian/Turonian	silt, clay, some volcanics	A*
Hatteras	Cenomanian (mid-Cretaceous to Barremian)	limestone, claystone	β^1
Blake-Bahama	Barremian (Early Cretaceous) to Tithonian	white-gray laminated chalk, bioturbated chalk and limestone, calcareous siltstone, claystone	β C ¹
			C
Cat Gap	Tithonian (Late Jurassic) to Oxfordian	grayish-red calcareous claystone	D ¹
		limestone, turbidites and greenish claystone	
unnamed	Oxfordian (Late Jurassic) to Callovian (mid-Jurassic)	variegated reddish to greenish claystone, limestone turbidites, dark claystone, greenish red claystone, blackish claystone, reddish claystone	D
BASEMENT		BASALT	BASEMENT

seismic reflection records reveal a steplike escarpment (Klitgord and Grow, 1980) north of the Blake Outer Ridge, and a broad hump south of it (Markl and Bryan, 1983). A schematic representation of this basement change is shown in Figure 6.

Basement relief (valleys and ridges) also is associated with fracture zones, even in cases where little or no offset has occurred (Detrick and Purdy, 1980). Three major fracture zones (Blake Spur, Jacksonville, and Bahamas)

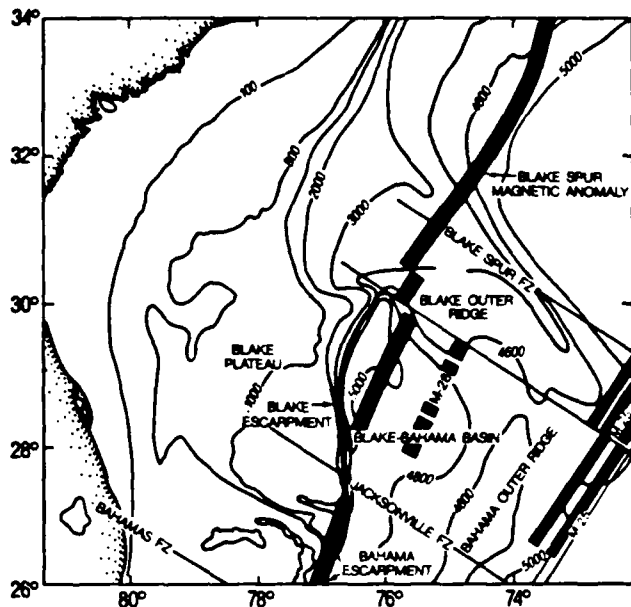


Figure 5. Locations of magnetic anomalies and fracture zones (Klitgord et al., 1984; Bryan et al., 1980; and Shouten and Klitgord, 1977) near site 534. Contours are in meters.

and at least one smaller zone cross the Blake-Bahama Basin from northwest to southeast (Perry et al., 1981; Klitgord et al., 1984) (Fig. 5). Some degree of basement relief can be expected in the vicinity of these fracture zones.

Major reflectors above basement have been recognized throughout the western North American Basin. Jansa et al. (1979) synthesized data from DSDP drill holes in the area and established a system of identification for the geologic formations. Table 2 shows the formation names, ages, and lithologies. Also shown are the approximate locations within the stratigraphic column of the reflectors that produce seismic horizons M through basement. The geologic explanations, or causes, for some of these reflectors have not definitely been established. Also, depending on the geographic location, different explanations may be linked with the same reflector. Thus, the associations between reflectors and formations shown in Table 2 should be considered tentative.

The mid-Jurassic deposits in the incipient Atlantic Ocean are terrigenous sediments and reworked calcareous debris, the latter probably derived from coral reefs. These deposits were first recovered at site 534 and have not been assigned a formation name. By late Jurassic time, about 150 million years ago, the sediments were mainly pelagic. The Cat Gap formation, for example, contains argillaceous limestones and claystones.

Similarly, the Blake-Bahama formation is composed of limestones, chalks, claystones, and some chert beds. These sediments were deposited near the end of the Jurassic and beginning of the Cretaceous, or about 145 to 120 million years ago.

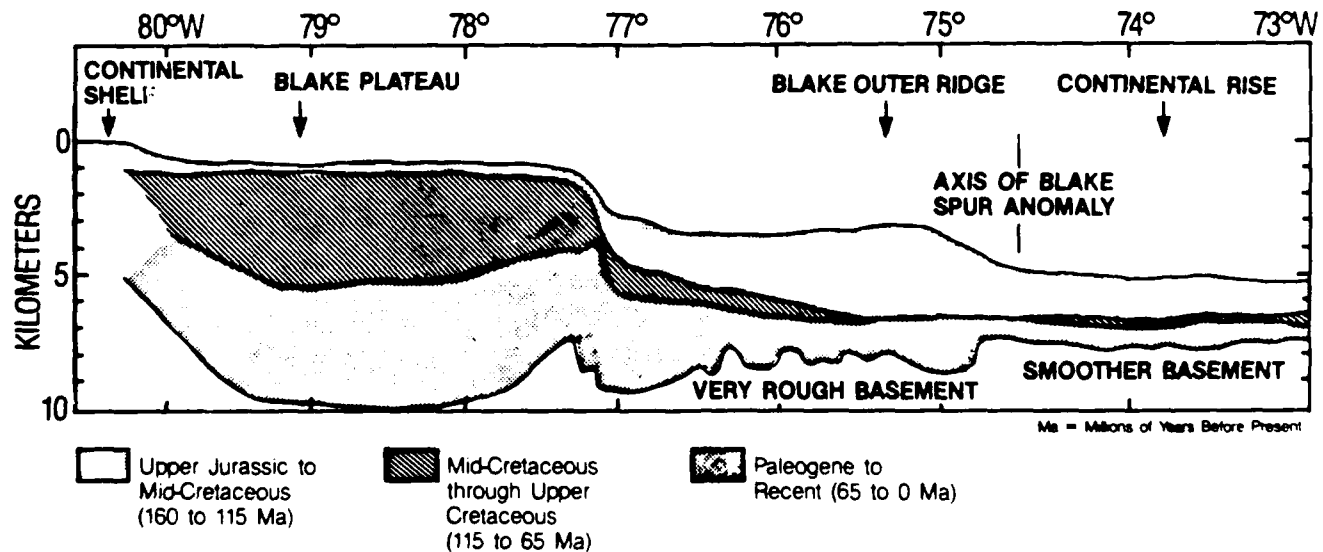


Figure 6. Change in basement structure at location of Blake Spur Magnetic Anomaly and sedimentation patterns across the Blake Plateau and the Blake Outer Ridge (modified from Shipley et al., 1978). Location of cross section is shown in Figure 1.

The mid-Cretaceous Hatteras formation records an anoxic environment during which there was widespread deposition of black clay. The clay is overlain by late Cretaceous to late Paleocene multicolored pelagic clays of the Plantagenet formation. Within the formation a lithologic change occurs at about Maestrichtian time. On seismic reflection records, this change is correlated with the lowest subdivision of horizon A (Ewing and Ewing, 1962; Ewing and Ewing, 1963) or horizon A* (Tucholke and Mountain, 1979).

Above Plantagenet is the Bermuda Rise formation, which is also characterized by turbidites, clays, oozes, and chert beds. The cherts were identified as horizon A reflectors (Ewing et al., 1970), and are now classified as horizon A subdivision A^c by Tucholke and Mountain (1979). This formation is early mid-Eocene in age, or about 52 to 45 Ma.*

The uppermost formation, the Blake Ridge, consists of mixed terrigenous and biogenic (pelagic) sediment, much of it deposited by turbidity currents emanating from the continental margin. Away from the margin in the more open portion of the Blake-Bahama Basin, the Blake Ridge Formation overlies the Bermuda Rise Formation and therefore is mid-Eocene to Recent in age. Near the continental margin, however, the Blake Ridge is Miocene to Recent in age because late Eocene and Oligocene sediments have been eroded. In this region, then, the Blake Ridge Formation unconformably overlies the Bermuda Rise Formation and sometimes older strata (i.e., Plantagenet, Hatteras). The unconformity is observed on seismic reflection records as Horizon A^u; farther seaward the base of the Blake Ridge Formation correlates with Horizon A^c.

B. Seismic Stratigraphy

DSDP holes and thousands of kilometers of seismic reflection coverage have provided data for generalized seismic stratigraphic correlations in the western Atlantic. The seismic stratigraphy described here is taken from Tucholke and Mountain (1979) and Sheridan et al. (1983).

Members of the shipboard party on DSDP leg 76 disagree about the stratigraphic correlations for four of the reflectors observed at site 534. Slightly different assumptions about velocities and the location of the hole relative to seismic profiles account for the differences. We chose the correlations of Sheridan et al. (1983) because they are representative of the correlations generally accepted by scientists working in the area; however, Table 3 presents both the correlations

of Sheridan et al. (1983a) and of Shipley (1983). It must be kept in mind that no unique identification of deep reflecting horizons is yet possible. The seismic stratigraphic correlations made at site 534 are shown in Table 3 and in Figure 7. The association between the geology and identified seismic horizons follows:

- Horizon D: Oxfordian (Jurassic) age, underlying sediments are limestone interbedded with claystone; these basement-leveling sediments were ponded by the BSMA Ridge, but extend beyond the ridge as streamers in the fracture zone valleys.

- Horizon D': represents a change from turbidite limestones to claystones within the Kimmeridgian (Jurassic) age sediments of the Cat Gap formation.

- Horizon C: marks the top of a calcareous claystone of Tithonian (Jurassic) age.

- Horizon C': caused by an abrupt boundary between limestones and claystones within the Berriasian (lower Cretaceous); the break might be indicative of a nondepositional hiatus.

- Horizon b: at site 534 it represents the top of an early Cretaceous, white turbiditic limestone.

- Horizon b': correlated with the boundary between the Aptian-Albian (mid-Cretaceous) multicolored claystones and the overlying black and green claystones, which represent a time of stagnation during Albian time.

- Horizon A^c: caused by a thin layer of Eocene chert; in the vicinity of hole 534 the reflector merges with the A^u reflector.

- Horizon A^u: represents an unconformity; erosion by bottom currents some time during late Eocene to early Miocene truncated sediments down into the Plantagenet formation.

- Horizon X: was first identified from profiles on the Outer Ridge (Markl et al., 1970); represents the boundary between interbedded chalks and mudstones and interbedded turbidites and claystones of lower-Miocene age. Within horizon X, Markl and Bryan (1983) recently identified subhorizons Xa through Xe.

- Horizon M: represents upper Miocene debris flows and chalk turbidites.

Although there are some notable exceptions, the sediments recovered at sites 391 and 534 are generally similar. One major difference is the absence of the Eocene siliceous claystone and chert in hole 391, while they constitute a 27-m-thick layer in hole 534. This difference indicates how much lithologies can vary laterally over a short distance (22 km in this case). Most of the correlation problems between the two sites, however, are the result of partial core recovery, not geologic complications. Figure 8, taken from Sheridan et al. (1983b) correlates reflecting horizons in site 534 with those of site 391. The reflectors are continuous between the two sites, but in some places their character is different and the depth to some reflectors changed by more than 100 m over the 22 km between the sites.

*The abbreviation Ma (megannum) refers to units of $\text{yr} \times 10^6$ measured from the present (AD 1950 by international agreement) pastward. It means the same as the cumbersome millions of years before present and is a fixed chronology analogous to the calendars tied to historical events. The abbreviation m.y. (million years) is used to express simple duration in units of $\text{yr} \times 10^6$ in any given past interval.

C. Geologic Factors Impacting Seismic Propagation

Some environmental features of the study area can be expected to complicate seismic propagation predictions. Among the most obvious are the following:

1. **Basement Relief and Crustal Structure:** The site is located on an east/west-trending rise (Fig. 3). To the south is a depression believed to be produced by

a small fracture zone. As noted, studies of fracture zones indicate greater relief in the basement adjacent to a fracture zone. Furthermore, recent findings indicate that the thickness of the crust may not necessarily be the same at fracture zones as it is in the regions between them. North Atlantic seismic data suggest differences in crustal thicknesses and velocities in the regions of fracture zones (Mutter and Detrick,

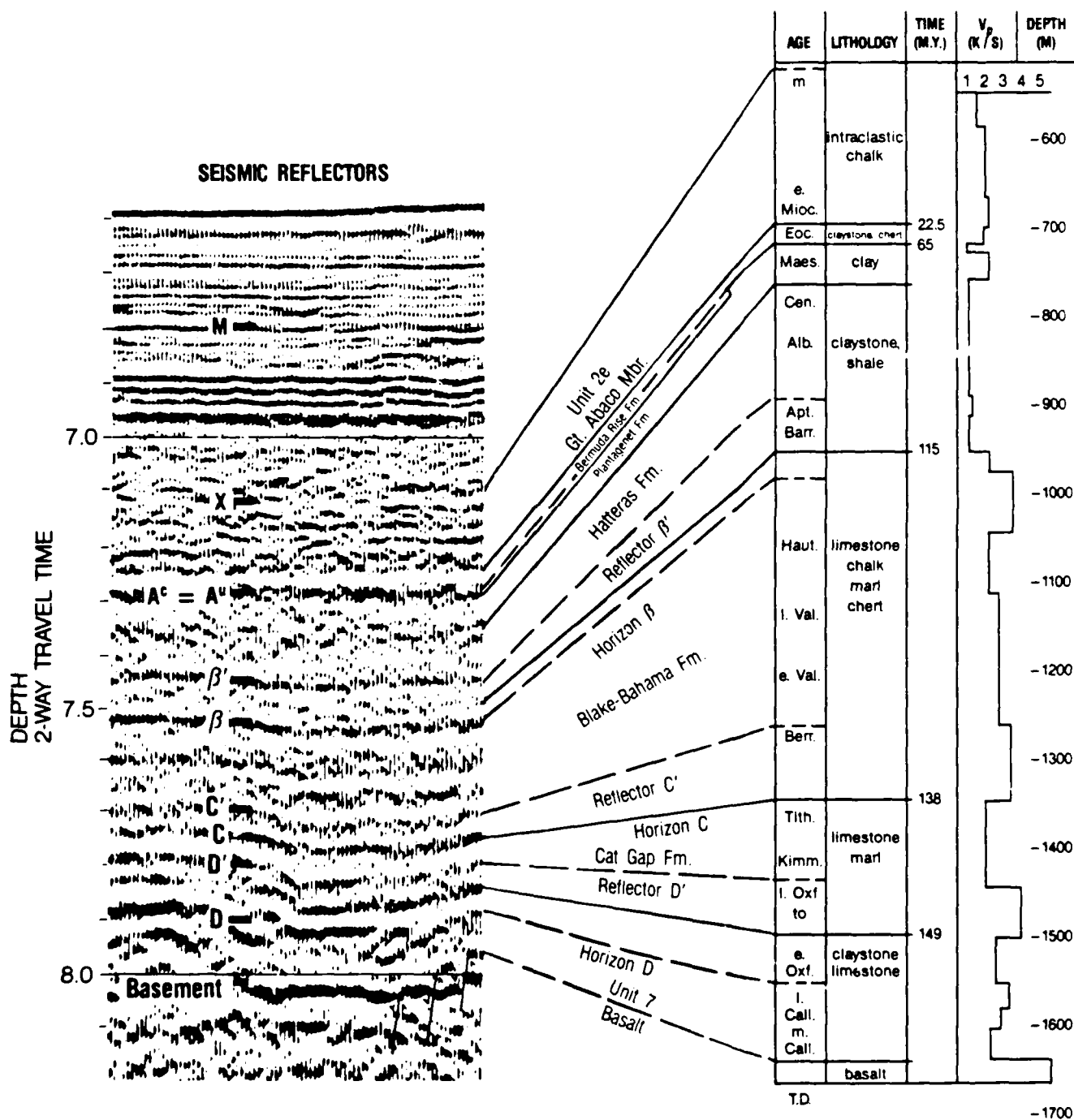


Figure 7. Correlation of seismic reflectors with geologic units at site 534. Reflecting horizons M, X, A', β', β, C', C, D', D, and basement are shown. Correlations and velocity profile are from Sheridan et al. (1983a). Velocities used for the profile are laboratory measurements on cores from hole 534A. Figure adapted from Sheridan et al. (1983a).

1984; Detrick and Purdy, 1980). Reflections from what Mutter and Detrick (1984) determine to be Moho (the crust-mantle transition depth) indicate that the oceanic crust at the Blake Spur Fracture Zone, about 500 km to the east of site 534, may only be about 2 to 2.4 km thick.

The Blake Spur Fracture Zone is wider and more distinct on bathymetric charts than the fracture zone near site 534 but both exhibit very little offset. Because

they differ in size the two might not be comparable; nevertheless, the crust near site 534 could be anomalously thin.

2. Lateral Variability: Deposition and erosion patterns mainly control the physical character of lithologic units. Although a unit may be acoustically traceable (i.e., a reflector) over a long distance, the geologic conditions that produced the unit may have changed substantially over the same distance. The change(s) can

Table 3. Correlations of seismic reflectors with geologic boundaries from DSDP holes 391 and 534.

REFLECTOR	DEPTH BELOW SEA FLOOR (km)		LITHOLOGIC DESCRIPTION		FORMATION		AGE	
	1	2	1	2	1	2	1	2
M (site 391)	.2		Intraclastic chalk		Blake Ridge		mid-Miocene	
X (site 391)	.5		mudstone/chalk		Blake Ridge		Early Miocene	
A ^u	.7		unconformity				Late Eocene-Early Miocene	
A ^c	.7		chert/siliceous claystone		Bermuda Rise		Late Eocene	
β'	.9		unconformity/claystones		Hatteras		Aptian/Albian	
β	.98	.95	turbidite ls.	chalk	Blake-Bahama		Hauterivian	Barremian
c'	1.25	1.2	ls-claystone boundary	chalk	Blake-Bahama		Berriasian	Valanginian
c	1.34	1.27	calcareous claystone	chalk-ls boundary	Cat Gap	Blake-Bahama	Tithonian	Berriasian
D'	1.43	1.34	turbidite ls/claystone	calcareous claystone	Cat Gap	Cat Gap	Kimmeridgian	Berriasian
D	1.55		increased ls content		unnamed		Oxfordian	

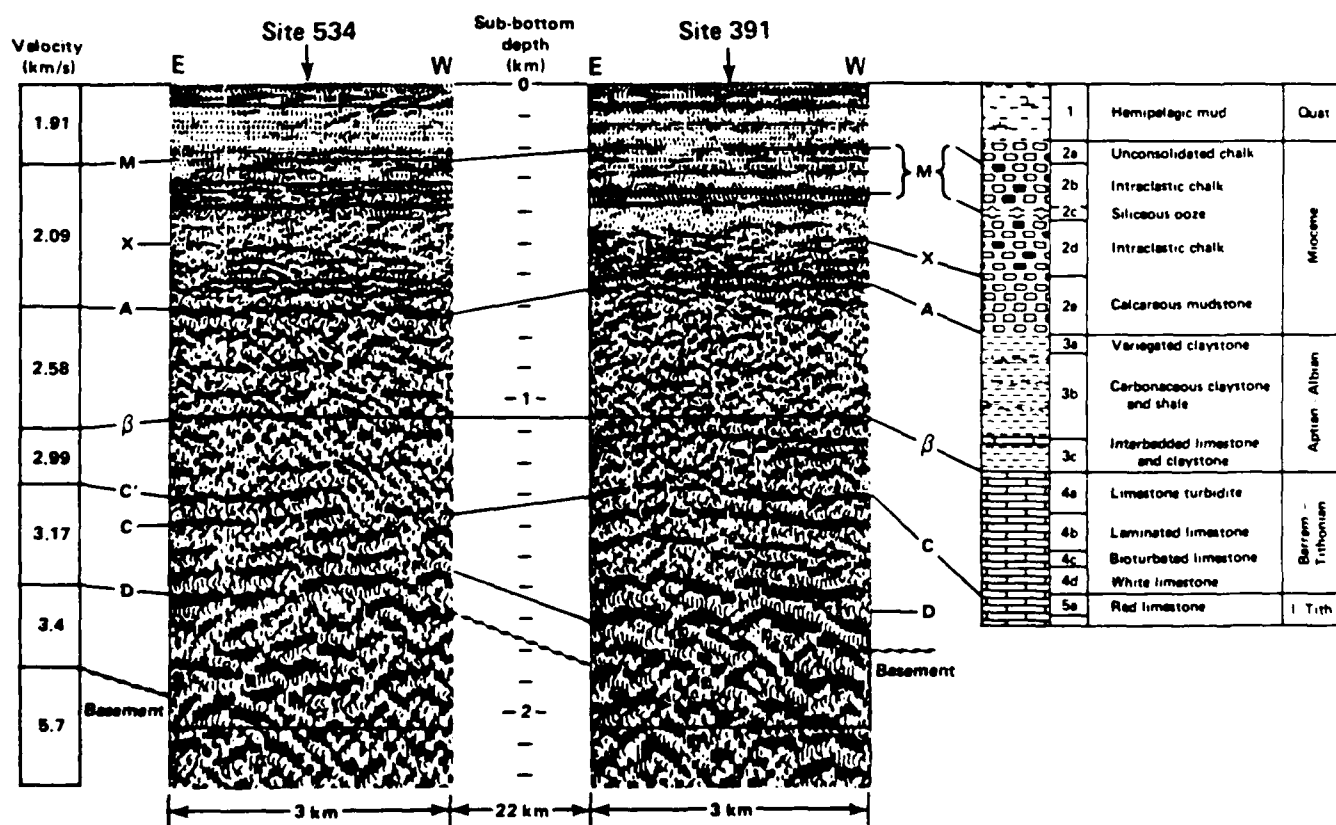


Figure 8. Correlation of seismic reflection records at site 534 and site 391; also shown are the correlations of the reflectors with geologic formations and the interval velocities, calculated assuming these geologic correlations.

result in lateral fluctuations in the physical properties of the unit or even its absence at some places. Although, as noted, the sedimentary columns at sites 391 and 534 are similar, the significant absence of chert at site 391 illustrates that even prominent lithologic units may be horizontally discontinuous. In the Blake-Bahama Basin, deposition and erosion were strongly influenced by the location of the Gulf Stream and other early Atlantic circulation patterns.

3. Small-scale Sea Floor Relief: The presence of small-scale topography at the site is indicated by hyperbolic echoes on the bathymetry records. As will be discussed, small-scale relief may complicate the acoustics in an area.

4. Ocean Currents: As discussed in section VII of this report, eddy currents with orbital speeds of about 40 cm/sec have been observed in the Blake-Bahama Basin. One comment from the DSDP site 534 report (Sheridan et al., 1983b) is particularly significant in this case. "The end of the drill string with approximately 40 tons of casing attached was very sluggish in its movements toward the reentry cone. Movement was resisted until the *Glomar Challenger* was offset over 30 m. Even with these offsets, the pipe swung very slowly and was apparently out of phase with ship movements. It was thought the inertia of the extra casing weight was acting as an anchor. Now bottom currents at site 534 are postulated to explain the pipe drag."

D. Velocity and Density Profiles

Physical properties measurements were not made on the upper 545 m of sediment from hole 534A because the sediments were considered very similar to those at site 391 (Sheridan et al., 1983b). Plots of compressional wave velocity and density as a function of depth for the sediments from both sites are presented in Figure 9. Listings of the data used to generate the plots are included in Appendix A-1. The sources of these data are the DSDP reports for site 534 (Sheridan et al., 1983b) and site 391 (Benson et al., 1978).

III. Area II: Nares Abyssal Plain (DSDP Holes 417/418)

A. Geologic Setting

DSDP sites 417 and 418 are located just south of the Bermuda Rise, between the Nares and Hatteras Abyssal Plains (Fig. 1). Water depth (Fig. 10) is generally between 5400 and 5700 m, with a few localized prominences rising to as shallow as 4900 m depth. Oceanic basement is found about 200 to 400 m beneath the sea floor. Basement relief in the area is 200 to 500 m.

The primary purpose of drilling at sites 417 and 418 was to study older (i.e., greater than 100 million years)

oceanic crust. Previous sampling had been done closer to the mid-Atlantic Ridge; the samples from sites 417 and 418 would be used to define changes in properties of the oceanic crust with age. The holes were drilled

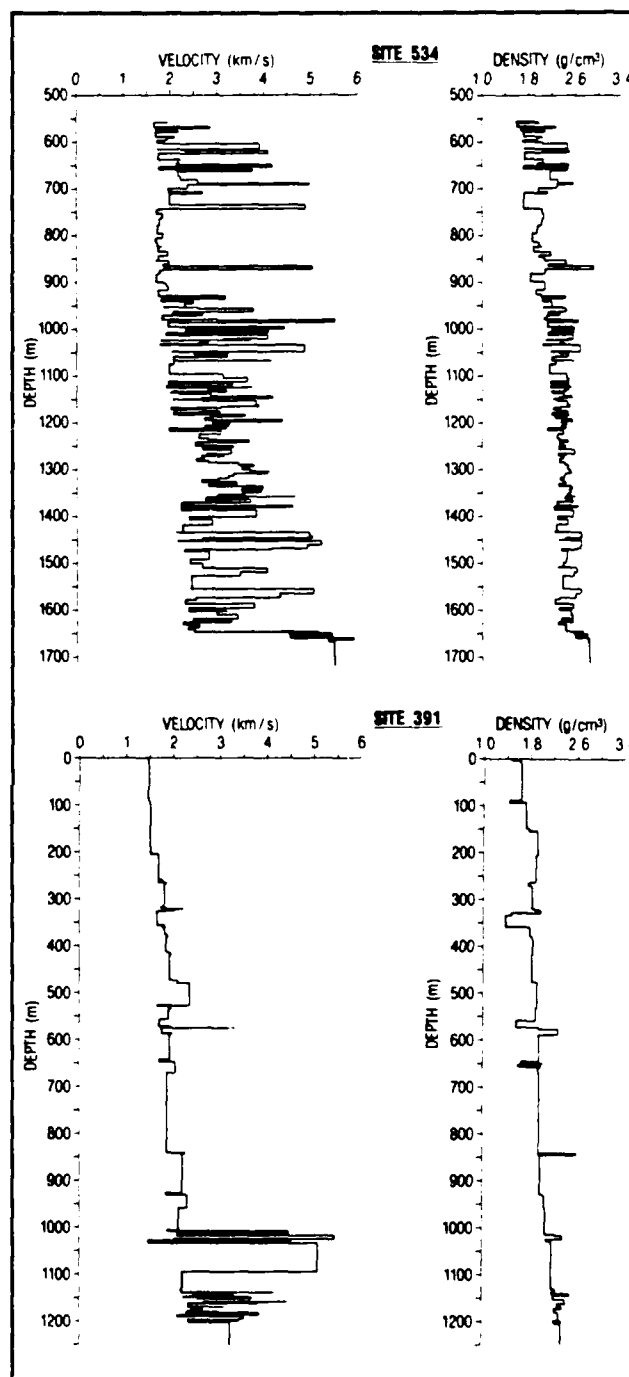


Figure 9. Velocity and density as functions of depth for DSDP sites 534 and 391. The data used to make these plots (Appendix A-1) are shipboard laboratory measurements of velocities and densities for samples at the given depths in the cores. No correction has been made for sediment rebound and no consideration has been given to sediment not recovered in the cores. The recovery rate for hole 534 was 56% and for hole 391 was 50.1%.

into oceanic crust geographically located at the source of the M-0 magnetic lineation. The age of the crust and the oldest sediment at this site are about 108 to 109 million years (mid-Cretaceous, Aptian/Albian) (Childs, 1985).

At site 417 (Fig. 10) four holes, 417, 417A, 417B, and 417D were drilled. Holes 417 and 417B were pilot holes. 417A was drilled into a basement high to a depth of 417 m below the sea floor — 209 m were in basalt, 208 m in sediment. Hole 417D was a multiple reentry hole that penetrated 533 m; 343 m of sediment and 190 m of basalt were drilled. The hole was reentered during leg 52 and an additional 175.5 m of basalt were drilled. The sediments at site 417 are typical of those found in the western Atlantic Ocean. The sedimentary history of the region is presented in section I of this report. At site 417A about 200 m of sediment (clay and ooze) were drilled before basement was reached; this sedimentary section is incomplete. In hole 417D, located about 600 feet west of 417A and off the basement hill on which 417A was located, an additional 100 m (approximately) of sediments underlie those drilled in hole 417A. These sediments are a multicolored clay, a black and green organic claystone with an interbedded sandstone/claystone turbidite sequence, and a thin chalk unit. The crustal basalt recovered from 417A was highly altered by exposure to seawater for as long as 30 million years before being buried by the overlying impermeable clay.

The objective of drilling at site 418 (about 6 km south of site 417) was to penetrate the basement deeper than it had been at site 417. The site is close to the eastern edge of the M-0 anomaly; is downslope from site 417; and is in an area of relatively flat, highly reflective basement with no prominent hills.

At site 418, 324 m of sediment and 246.5 m of basalt were drilled. The hole was reentered on leg 53 and an additional 297.5 m of basalt were drilled. The basalts are mostly fresh. Some pillow basalts contain lithified sediments that were apparently present on the sea floor at the time of eruption.

Hole 418B was drilled 130 m north of hole 418A in an attempt to recover more sediment than was recovered at hole 418A. The sediment section is similar to that at site 417. Figure 11 shows the sedimentary sections at sites 417 and 418.

B. Seismic Stratigraphy

Four strong reflecting horizons appear in the reflection records collected near sites 417 and 418 (Fig. 12). Their correlation with lithologic boundaries, suggested in the reports from DSDP sites 417 and 418, is unsatisfactory. Near hole 417A the fourth, or deepest reflector, is 0.24 sec below the sea floor and appears to represent the top of the basalt basement. This travel time and actual depth to basement indicate that the

sediments have an average velocity of 1.76 km/sec. However, measured velocities range from 1.50 to 1.65 km/sec. Reflector 1, the first observed below the sea floor, is correlated with a change in induration at 80 m in a pelagic clay. Reflector 2 at the site is masked by a strong bubble pulse. Reflector 3, at 0.175 sec below the sea floor, is correlated with the top of a

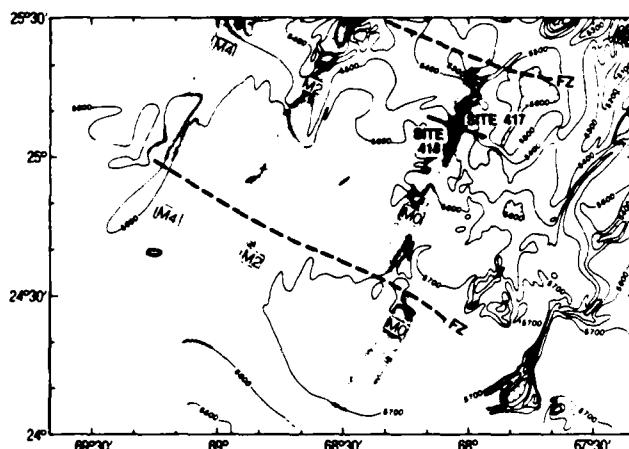


Figure 10. Bathymetry (contoured in meters) in the area surrounding DSDP sites 417 and 418. Dashed lines indicate locations of fracture zones. Locations of Mesozoic magnetic lineations, M-0, M-2, and M-4 are shown. Thick lines are the locations of the Oblique Seismic Experiment track lines (adapted from Stephen et al., 1980).

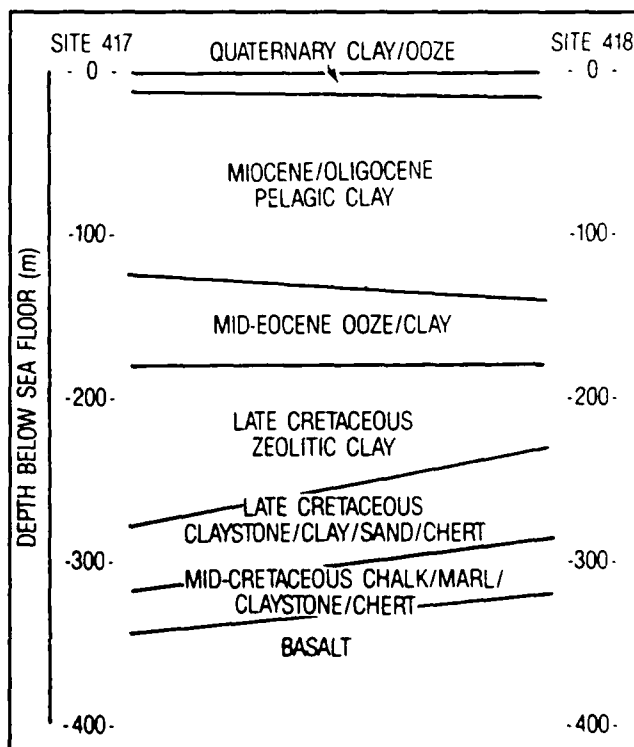


Figure 11. Generalized lithologic section showing the depth to various units at sites 417 and 418.

multicolored clay. If this last correlation is correct, then the velocity through the sediments above reflector 3 would be 1.83 km/sec, implying that the seismic velocity through the sediments between reflectors 3 and 4 is significantly lower than that above reflector 3.

At hole 417D the basement reflector is at 0.413 sec, suggesting that the velocity in the overlying sediment is 1.6 km/sec. This amount is different from the calculated interval velocity at hole 417A but similar to the laboratory-measured velocities for sites 417 and 418.

At site 418 the horizon at 0.4 sec is not distinct and is probably masked by overlying chert. The average velocity through the sediments should be 1.6 km/sec. A prominent reflector at 0.2 sec can be traced via the records to the area of 417D where it occurs at 0.18 sec. There, it is correlated with the top of the multicolored clay. At hole 418B the clay is at 177 m. This geometry produces sediment velocities of 1.77 km/sec for the sediments above 0.2 sec and 1.47 km/sec for those below. An alternative would be to correlate the 0.2-sec reflector with the top of a mid-Eocene zeolite clay. This correlation produces more acceptable velocities of 1.5 km/sec for the upper layers and 1.74 km/sec for the lower layers but does not agree with correlations at site 417.

C. Oblique Seismic Experiment

The Oblique Seismic Experiment (OSE) was conducted at site 417D. Because the bottom hole assembly had broken off and remained in the hole, the OSE was performed in the open section of the hole between 344 and 603 m subbottom. The instrument package consisted of a three-component geophone clamped to the walls 228 m into the basalt. Tovex extra explosive charges (20 lb) were detonated at approximately 46 m below the sea surface and at 0.5-km intervals along two perpendicular 12-km lines. The lines were centered at the drill ship (*Glomar Challenger*). Although intended to be north-south/east-west lines, they were actually slightly rotated clockwise as shown in Figure 10. The north-south line was repeated with the instrument package repositioned at 8 m into the basalt. All recording equipment was aboard the *Glomar Challenger*. The shooting ship was the *Virginia Key*.

Valuable information relating to acoustic propagation paths within the basement was provided by the OSE experiment. At the Mid-Atlantic Ridge the preferred north-south orientation of ridges, faults, and fissures caused velocity anisotropy between north-south and east-west-oriented lines. The OSE experiment showed that this anisotropy did not exist at site 417D, suggesting that cracks and fissures close with age. The constant change of velocity with depth suggests that the cracks close with depth as well as age (Stephen et al., 1980).

Stephen et al. also demonstrated the effect of small-scale basement topography on travel-time for the top of Layer 2 (upper level of oceanic basement). Their efforts to study velocity anisotropy were hampered by the obvious effect of small-scale topography. The regional scale topography had been determined using standard profiler techniques and was incorporated into their calculations. Figure 13 is a plot of the difference between the calculated arrival time using regional topography corrections and an assumed velocity of 4.8 km/sec, and the actual arrival time. The residuals shown in Figure 13 (taken from Stephen et al., 1980) indicate that the topography is rougher when perpendicular to the magnetic lineations than when parallel to them. Stephen et al. state, "There is no point in studying lateral velocity effects from direct arrivals unless the small-scale topography is known accurately from detailed profiling."

Velocity averages obtained by the OSE were found to agree better with velocities obtained by well logging at site 417 than with laboratory measurements (for example, 4.8 km/sec vs. 5.4 km/sec in basalts). It is suggested that the reason for higher laboratory measurements is the presence of small cracks in the rock that occur on a scale larger than the size of the laboratory samples (Salisbury et al., 1980).

D. Geologic Factors Impacting Seismic Propagation

Some factors peculiar to this site could have an effect on acoustic transmission:

- The site is located between two fracture zones, one about 20 km to the north and the other about 70 km to the south. They are the result of small offset transforms and do not exhibit the relief seen along some major fracture zones. Previous comments concerning fracture zones at site 534 apply here also.
- During the OSE experiment Stephen et al. (1980) concluded that small-scale topography adversely affected their ability to predict seismic travel times.
- Hole 417A was drilled on a topographic high and contained the most altered basalts recovered from a DSDP borehole, to that date (1977). Mineral alteration will affect density and crystallography and, therefore, the geoaoustic properties. Hole 417A values for velocity and density in at least the upper 50 m of basement are lower than those of sites 417D and 418. Other hills in the area could have altered mineral sites.

E. Velocity and Density Profiles

A listing of the laboratory measurements of seismic velocity, density, and porosity values for each sample from sites 417 and 418 is presented in Appendix A-2. The measurements from holes 417A, B, and D were

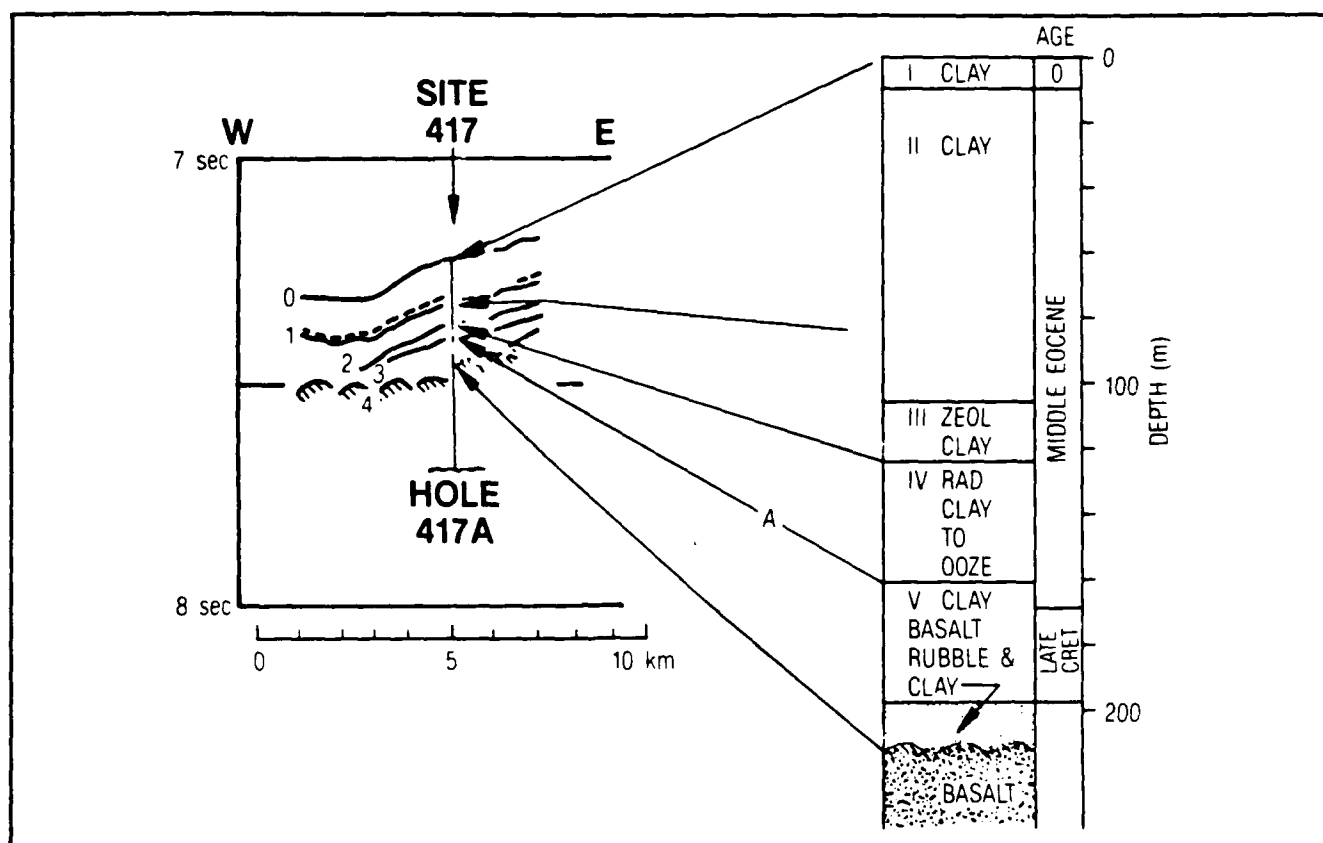


Figure 12. Correlation of four strong reflectors with possible lithologic reflecting horizons at site 417 (adapted from Donnelly et al., 1980). ZEOL indicates zeolitic and RAD indicates radiolarian.

combined to construct a complete sedimentary section. The measurements from the basalts include data collected to a depth of 500 m below the sea floor. Plots of laboratory-measured seismic velocity and density vs. depth for sediments from sites 417 and 418 are presented in Figure 14.

IV. Area III: Blake Plateau

A. Geologic Setting

The Blake Plateau is located off the coast of the southeastern United States, roughly between 27°N and 31°N, and at water depths of 600 to 1000 m. It is bounded on the west by the Florida-Hatteras slope and on the east by the Blake Escarpment. Because this 125,000 km² portion of sea floor is located between continental shelf and oceanic depths, it is considered to be an anomalous feature and has been intensely studied.

Crystalline basement is covered by as much as 13 km of unconsolidated and consolidated sediment (Fig. 15). The northern part of the plateau is underlain by the Carolina Trough, a deep, elongated basement feature extending from about Cape Hatteras to 31°N under the continental slope. The remainder of the plateau is underlain by the bowl-shaped basement of the Blake Plateau Basin.

Figure 16 is a generalized profile across the plateau at 28°N and depicts the basic history of sedimentation on the plateau. Velocities indicated in the figure were obtained from a multichannel seismic profile across the plateau.

Initial rifting of the continental crust in this area probably began in late Triassic time. Triassic and possibly early Jurassic volcanoclastic and terrigenous sediments began to fill the basement rifts. During Jurassic time the area subsided and was covered by the

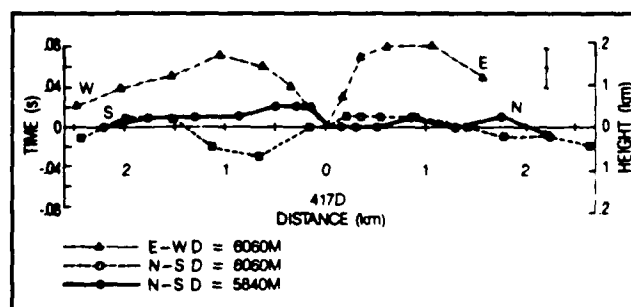


Figure 13. Travel time residuals: differences between observed travel times and those calculated assuming a layer 2 (basement) velocity of 4.8 km/sec and regional topography from bathymetric profiles. D indicates the depth of the geophone below the rig floor. E-W and N-S refer to the east-west and north-south OSE tracklines shown in Figure 10.

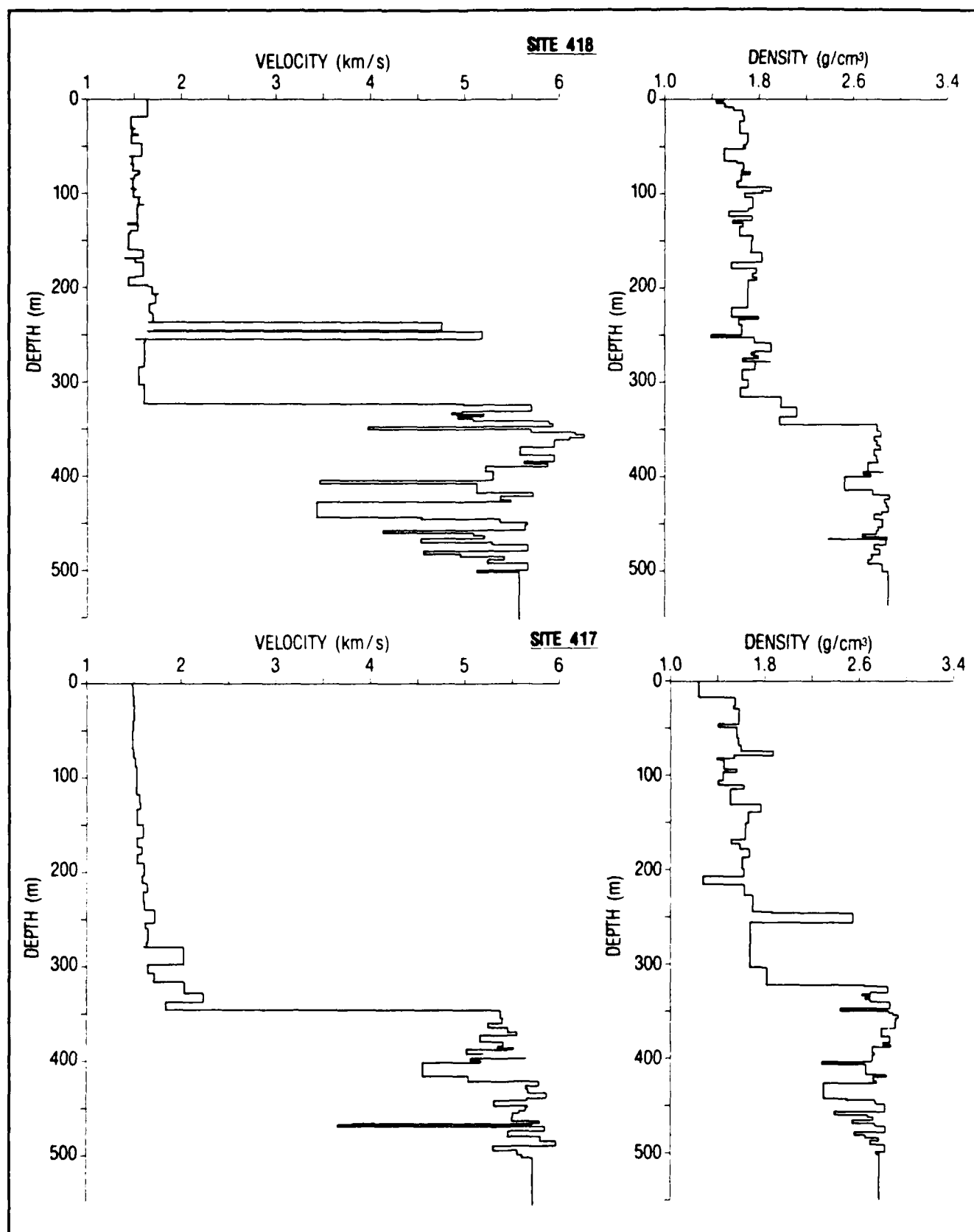


Figure 14. Plots of velocity and density vs. depth for shipboard laboratory-measured samples from sites 417 and 418. No correction has been made for rebound of sediments and no consideration has been given to sediment not recovered in the cores.

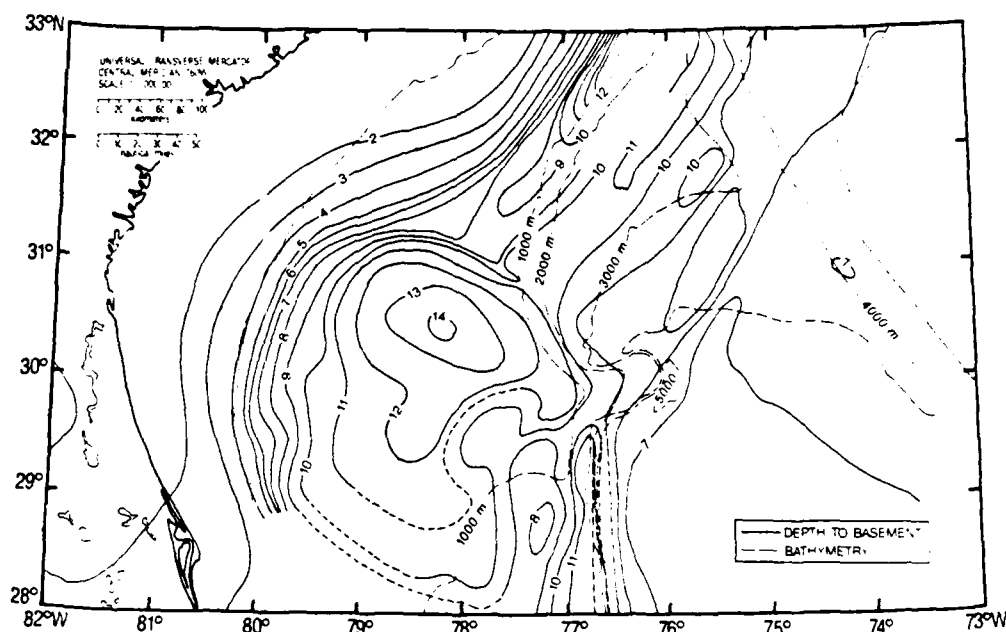


Figure 15. Contour map of the Blake Plateau showing bathymetry in meters and the depth to basement in kilometers (adapted from Popenoe, 1984).

ocean. Reef growth occurred along the edge of the continually subsiding Blake Plateau. Landward of the reefs, limestone deposits accumulated until the mid-Cretaceous. Additional subsidence and a rise in sea level brought deep-water deposits to the plateau. During the early Eocene the Gulf Stream began to flow through the area, causing long periods of nondeposition and scour, which accounts for the fact that the remainder of the sedimentary column on the plateau is so much thinner than that of the continental shelf to the west.

A detailed seismic stratigraphy of the upper kilometer of sediments was presented by Pinet and Popenoe (1985). By correlating their single-channel seismic reflection lines with those collected on the shelf and the plateau (Dillon et al., 1979), and with drill holes on the plateau, they were able to correlate reflectors with sediments of mid-Cretaceous through Oligocene age. Only small pockets of post-Oligocene sediments are identified on the records.

B. Geologic Factors Impacting Seismic Propagation

Although the presence of a singular rock type (limestone) with a thickness of about 7 to 12 km might seem ideal for modeling, the character of the limestone must be considered. At the edge of the Florida/Georgia shelf, for example, the limestones are lithified coral reefs, which are generally recognized on seismic reflection records by the absence of coherent signals rather than by strong signal returns. Also, on mainland

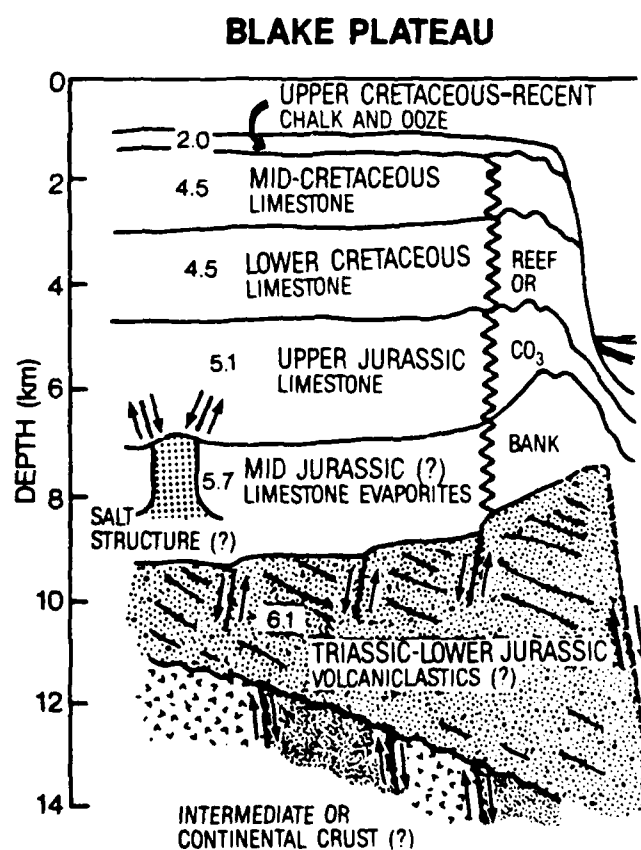


Figure 16. Schematic representation of the lithologic units and their compressional velocities across the Blake Plateau (after Sheridan et al., 1981).

Florida, sink holes found in limestone formations are the same, or similar, to those under the Blake Plateau. Although the depth of the limestones on the plateau implies that they are highly compacted and presently should not contain cracks, fractures, or solution features, previous in-filling of such features would produce a nonhomogeneous limestone.

Seismic records suggest the presence of lenses of different composition within the Blake Plateau limestone section (Sheridan et al., 1981; Shipley et al., 1978). Because diapirs, assumed to be composed of evaporites (salt), occur near the edge of the continental shelf farther to the north, it would not be unreasonable to expect salt lenses within the limestones of the Blake Plateau. For this reason, a salt dome is shown in Figure 16. The physical properties of salt are significantly different from the limestone (e.g., low density). Geophysically, salt is identified by its high compressional velocity.

At the landward edge of the Carolina trough, growth faults are generated as the sediments adjust to the movement of deeply buried evaporites which, in turn, are responding to the overburden pressure of the shelf sediments (Dillon et al., 1982). Some of these faults are under the Blake Plateau, and some faulting may occur farther south on the plateau in response to movement of evaporites.

North of 30°N large surface areas of the Blake Plateau are covered with a crust composed of phosphorite and manganese. The crust is generally less than 10 cm thick, but should be strongly reflective to high-frequency signals.

Gas hydrates are continually being discovered at continental margins around the world and have been found at the northern end of the Blake Plateau (Dillon et al., 1980; Paull and Dillon, 1981; Markl et al., 1970). Although little is known about their effect on acoustic propagation, their appearance on seismic records is clearly dramatic.

The Jurassic and Cretaceous age limestones of the Gulf of Mexico are prolific hydrocarbon source rocks. Thus, modeling of the Blake Plateau must also take into account the possible presence of oil and gas in the limestone.

Sediment scouring on the plateau will cause surface relief capable of scattering acoustic energy. In addition, the currents of the Gulf Stream can be a source of flow and turbulent noise.

V. Area IV: Bahama Platform

A. Geologic Setting

Area IV on Figure 1 is only the northwest portion of the Bahama Platform. The entire platform, extending to the southeast, covers 300,000 km² and is bordered on the south by the islands of Cuba and

Hispaniola, on the west by the state of Florida, on the north by the Blake Plateau, and on the east by the Bahama Escarpment. The platform consists of several shallow banks capped by 20 islands and over 3000 small cays. More than 200,000 km² of the platform are shoaler than 20 m. Deep water, in some places in excess of 1500 m, is found in the channels that dissect the platform.

The geologic history of the Bahama platform is similar to that of the Blake Plateau, except that persistent shallow-water carbonate buildup on the platform has resulted in the formation of the Bahama Banks and Islands. About 2.5 km of volcanoclastic sediments of Triassic and early Jurassic age overlie a basement of rifted transitional crust. Limestone, dolomite, and evaporite rocks, which comprise the next 3.5 km of the lithologic column, range in age from late Jurassic to mid-Cretaceous. The oldest carbonates under the Bahama Platform, therefore, are younger than the oldest carbonates under the Blake Plateau. The post-Albian transition to deep-water chalks and oozes is similar to that of the Blake Plateau. At times of higher sea level during the Pleistocene the present area was covered by water and oolitic limestone was deposited. Carbonate buildup continues on the banks today. Diagenesis of carbonate sands and muds to dolomite is also widespread because of reaction between the carbonate and hypersaline, magnesium-rich, seawater (brines). The process is enhanced by sea-level changes that have exposed subsurface rocks alternately to subaerial and submarine environments. Dolomite was drilled as shallow as 26 m below the surface in a bore hole on Grand Bahama Island (Paulus, 1972).

B. Geologic Factors Affecting Seismic Propagation

The character of the carbonates here is similar to that on the Blake Plateau. Inhomogeneities within the carbon rocks and surface relief on the platform will complicate transmission, as may fractures and mineralization associated with faulting at Northwest Providence Channel and the Great Abaco Canyon.

VI. Area V: The Bermuda Rise

A. Geologic Setting

The Bermuda Rise is a northeast/southwest-trending elongate arch approximately 2000 x 1000 km in size, located about 1500 km off the southeastern coast of the United States. The rise shoals to approximately 4000 m, or about 1 km shallower than the surrounding ocean basin. The Bermuda Pedestal, a flat-topped seamount on which the island of Bermuda stands, is located at about the center of the rise. Figure 17 shows the Bermuda Rise and the locations of DSDP drill sites 386 and 387.

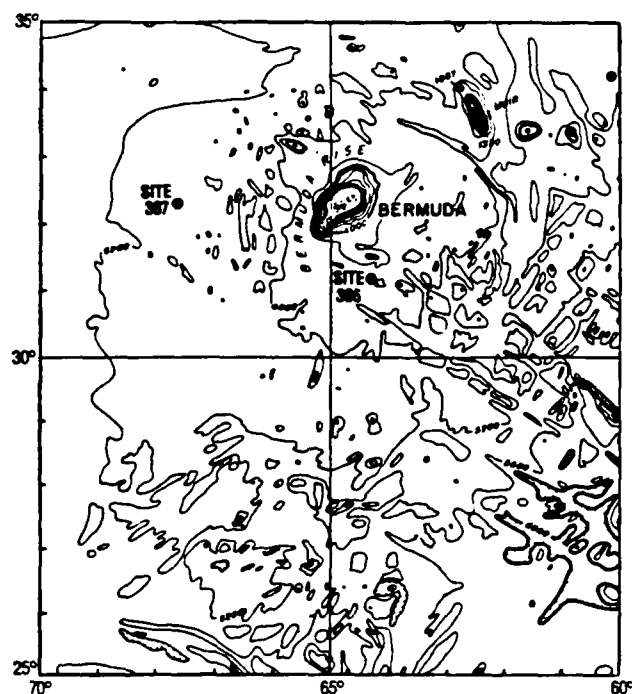


Figure 17. Contour map of a section of the Bermuda Rise. Locations of DSDP holes 386 and 387 are indicated.

B. Seismic Stratigraphy

Oceanic layer 2 is generally regarded as acoustic basement in the area. Basement is rugged, with features as shallow as 1.2 sec above the sea floor and as deep as 1.5 sec (two-way travel time) beneath it. The age of the crust at DSDP site 387 is early Cretaceous, or about 135 mybp, and is mid-Cretaceous, or about 105 mybp at DSDP site 386 (Childs, 1985).

The thickest sediments (1.5 sec) occur as an apron around the base of the Bermuda Pedestal. Away from the apron sediment thickness decreases. The Cretaceous-to-Recent geologic history is basically the same as that of the North Atlantic Ocean (presented in section I of this report), except that the post-Paleocene sedimentation and morphology has been significantly influenced by the formation of the Bermuda Rise.

The basal sediments are limestones and chalks of early Cretaceous age. The boundary between them and the overlying mid-Cretaceous black clays appears to correlate with the β reflector in seismic profiles (Tucholke, 1979). The black clays are overlain by red clays, followed by a late Cretaceous calcareous claystone and chalk unit (Fig. 18) that was correlated with the A* reflector (Tucholke et al., 1979).

On the Hatteras Abyssal Plain and on the western part of the Bermuda Rise, horizon A* is less than 0.1 sec below horizon A^c, and is often indistinguishable from A^c. East of 67°W, however, the two reflectors

LITHOLOGY	DEPTH	VELOCITY	REFLECTOR
HEMIPELAGIC CLAY	-0-	1.66	
MUD	-100-		
TURBIDITES	182 -200-		A ^t
	224		A ^c
CHERTY CLAYSTONE, MUDSTONE	-300-	2.01	
	-400-		
MARLY CHALK			
	470 -500-		A*
CLAYSTONE		1.75	
	-600- 610		β
CHALK AND LIMESTONE	-700-	2.08	
	792 -800-		B
BASALT			

Figure 18. Generalized lithology, seismic velocity, and depth to reflecting horizons at DSDP site 387. Depths are in meters and velocities in kilometers/second.

diverge and are easily recognized. They are about 500 to 600 m apart near Bermuda.

The Paleocene and early Eocene sediments are cherty claystones and mudstones that are overlain by mid-Eocene turbidites. Tucholke and Mountain (1979) relate the lower cherty unit to reflector A^c and the upper turbidite unit to A^t. Generally, when both reflectors are observed, the deeper reflector is the stronger and is recorded 0.1 to 0.2 sec beneath the other reflector.

In the area surrounding Bermuda, single-channel seismic records reveal a prominent reflector above A^v and A^c roughly midway in the sedimentary section. This reflector is designated A^v and correlates with the top of the late Eocene to mid-Oligocene volcanoclastic turbidites (Tucholke and Mountain, 1979). A^v forms an oval-shaped apron around Bermuda. Bowles (1980) indicates that it extends for 140 km in an easterly direction and from 210 to 225 km in a south-southeasterly direction.

A^v is observed on the seismic records obtained near site 386, but is not seen as far west as site 387 (Fig. 17). Near site 386, A^v is between 0.1 and 0.5 sec beneath the sea floor (two-way travel time).

Above horizon A^v the seismic records indicate that bottom currents were an important influence on sediment distribution. Bowles (1980) and Lowrie and Heezen (1967) demonstrated the strong tendency in the Bermuda area for surficial sediments to accumulate to the northeast of an obstruction, but sediment depletion is observed to the southwest.

Bowles (1980) also pointed out several areas around the base of the pedestal where records indicate the presence of ponded, acoustically laminated sediments deposited in depressions formed by current erosion during the Pleistocene. Laine (1978) also suggested that the weakly reflecting, acoustically laminated sediments, observed as the first set of subbottom reflectors, were deposited beginning in the early Pleistocene.

The transparent layer beneath these reflectors, which is presumably composed of Neogene pelagic sediments, thickens and thins independently of the underlying topography. This lack of conformity with the underlying surface suggests that currents redistributed the sediments (Bowles, 1980). Thus, Neogene sediment distribution throughout the area is unpredictable.

C. Geologic Factors Affecting Seismic Propagation

In this area there is considerable basement relief related to uplifting of the Bermuda Rise and the formation of the Bermuda volcano. Further, current scour and deposition have caused considerable topographic relief and give rise to the extreme variability in the sea-floor surface and near-sea-surface sediment types.

VII. Bottom Current Descriptions for 82°W-65°W, 23°N-33°N

Ocean bottom seismometer (OBS) performance can be adversely affected by bottom currents. Therefore, this section describes the variability and complexity of the bottom current circulation that exists in the western

North Atlantic in the vicinity of 23°N-33°N and 82°W-65°W.

A. Previous OBS Efforts

Ocean current noise is a problem for some ocean bottom seismometers. Duennebie et al. (1981) estimate that between 5% and 15% of OBS data taken by the Hawaii Institute of Geophysics were degraded by noise due to ocean currents. At short periods the principal mode of noise generation appears to be shedding of Karman vortices from antennas and other resonant obstructions. High-amplitude, narrow-band noise that correlates with periods of high (10 cm/sec) ocean bottom currents and the principal lunar semidiurnal tide (12.4 hours) has been observed.

Vortex shedding is not the only possible mode of coupling current-induced noise to OBS's. At long periods OBS tilting can be a serious problem. According to Duennebie et al. (1981) and Sutton et al. (1981), an instrument resting on soft sediment can be tilted by the pressure of the current exerted against it. Duennebie et al. gave an example of how an OBS, with a cross section of about 1 m in diameter centered about 0.5 m above the bottom with a tripod base and mass of 200 kg, would tip about 5×10^{-6} m (10^{-5} radians) in response to a 10-cm/sec current. This tilt would be sufficient to drive long-period seismometers off scale. Fluctuations about this 10-cm/sec current would produce objectionable noise at shorter periods. Boyd (1984) made near-bottom current measurements at DSDP Hole 395A (near 23°N-46°W). Marked spectral peaks at semidiurnal (12.4 hours) and inertial (30.7 hours) frequencies were measured. Mean and maximum current speeds of 4.4 and 9.0 cm/sec, respectively, were not strong enough to cause hydrodynamically generated noise; it is not certain however, that the seismic records were of high enough quality to separate background noise from induced noise (R. Jacobson, ONR/CRD, Washington, D. C.).

Figure 19 indicates the three sites for which a bottom description will be given. Generalized bottom sediment types (NAVOCEANO, 1965) are also shown for each area. Bottom depths range from less than 100 m in the northwest sector to more than 5600 m in the southeast sector.

B. General Deep Circulation

Neumann and Pierson (1966) describe the deep (3000 m) circulation as a mean southerly flow that extends down to about 5000 m in this region of the world; below this depth, Antarctic Bottom Water moves northward. According to Hogg (1983) the abyssal circulation in the western North Atlantic consists of two southerly components: one flows southwestward inshore of the 4000-m isobath; the other flows in deeper water farther offshore and recirculates

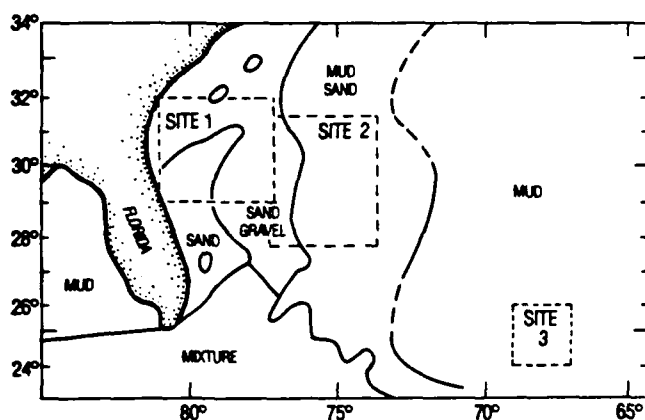


Figure 19. Generalization of bottom sediment types in the western North Atlantic around the sites (1, 2, and 3) where bottom currents are described.

water in a series of small, meridional-scale gyres. This concept was apparently first suggested by Schmitz (1977).

C. Circulation Variability

According to Webster (1971), long-term current measurements from different regions of an ocean show similar mean kinetic energy and mean speeds. At any given depth, less than a factor of two is present in the range of speeds. Webster (1969b) shows that deep-sea current spectra data are dominated by semidiurnal and inertial frequencies. Within this study area, the inertial period would vary from 30.7 hours at 23°N to 22.0 hours at 33°N.

Although the mean abyssal flow is low velocity (Amos et al., 1971), there is substantial variability in the circulation. Lai (1984) measured the Deep Western Boundary Current (DWBC) for over 100 days near the Blake Escarpment (28°N, 76°W). The width of the DWBC was about 60 km and its core of maximum velocity was located 10 km east of the escarpment. The mean flow was 22 cm/sec at 2500 m. Thirty meters above the bottom (4930 m), the mean flow decreased to 15 cm/sec. Higher speeds have been reported by Riser et al. (1978). Sound fixing and ranging (SOFAR) floats in the western North Atlantic, near the Blake-Bahama Outer Ridge (28°N-72°W), at depths between 1500 and 2000 m, were caught in an intense cyclonic eddy, which had a radius of 40 km and orbital speeds attaining 40 cm/sec. In the vicinity of the Blake Escarpment (28°N-76°W), Perkins and Wimbush (1976) also observed a cyclonic eddy that attained orbital speeds of about 40 cm/sec; the eddy diameter was approximately 60-80 km. Webster (1969a) stated that the time-dependent current components average each other out over long-period vector means, and that

the scalar mean speed can be two or three times as large. Kelley and Weatherly (1985) showed that energetic fluctuations can occur, even at near-bottom (4900 m) depths with time scales of 30 to 90 days. These fluctuations probably result from Gulf Stream meanders and rings. Both Gulf Stream and wind forcing may set up meanders with periods ranging from 1.4 to 12 days in shallow water (such as near the coast) (Li et al. 1985).

D. Best Estimate of Subsurface Currents

Wilcox (1978), Mills et al. (1981), NAVOCEANO (1964-1982), and others have provided comprehensive current meter records for several locations within the study area (Fig. 20). Wilcox developed a realistic data base of mean and maximum current speed for the design of deep ocean equipment. Short-term current meter records, as well as subsurface floats, were used to establish Wilcox's data base.

Figure 21 is a plot of mean and maximum current speed vs. depth for the stations shown in Figure 20. The most striking feature of the plot is the large scatter, which could be expected in such a diversified dynamic region. Figure 22 presents the data by "mean profiles"; note the large standard deviations associated with the curves.

An important consideration in site selection is the estimated variability of the current profile from area to area. Due to the large variability throughout the region, bottom depth was used as a primary selecting factor. Area 3 has the most consistent and deepest depths; therefore, the current variability and mean speeds should be less than for the other two areas (Fig. 22).

Typical near-bottom current speeds are estimated:

Area 1 - mean near-bottom speeds highly variable, as is bottom depth; mean speeds may vary between 5 and 25 cm/sec; strong rotary tidal influence present; expect maximum near-bottom speeds in excess of 25 cm/sec.

Area 2 - mean near-bottom speeds most likely do not exceed about 10 cm/sec; maximum speeds attain 25 cm/sec or less.

Area 3 - typical near-bottom speeds appear to be less than 6 cm/sec; maximum speeds are about 12 cm/sec.

E. Conclusions

Large variation in current speed and direction should be anticipated throughout the region. Below about 3000 m, current speed should decrease with increasing depth. Assigning mean current speed values to any one location based on historical data may not be meaningful because of the variability. At or near the bottom current speed and variability should be lowest in area 3,

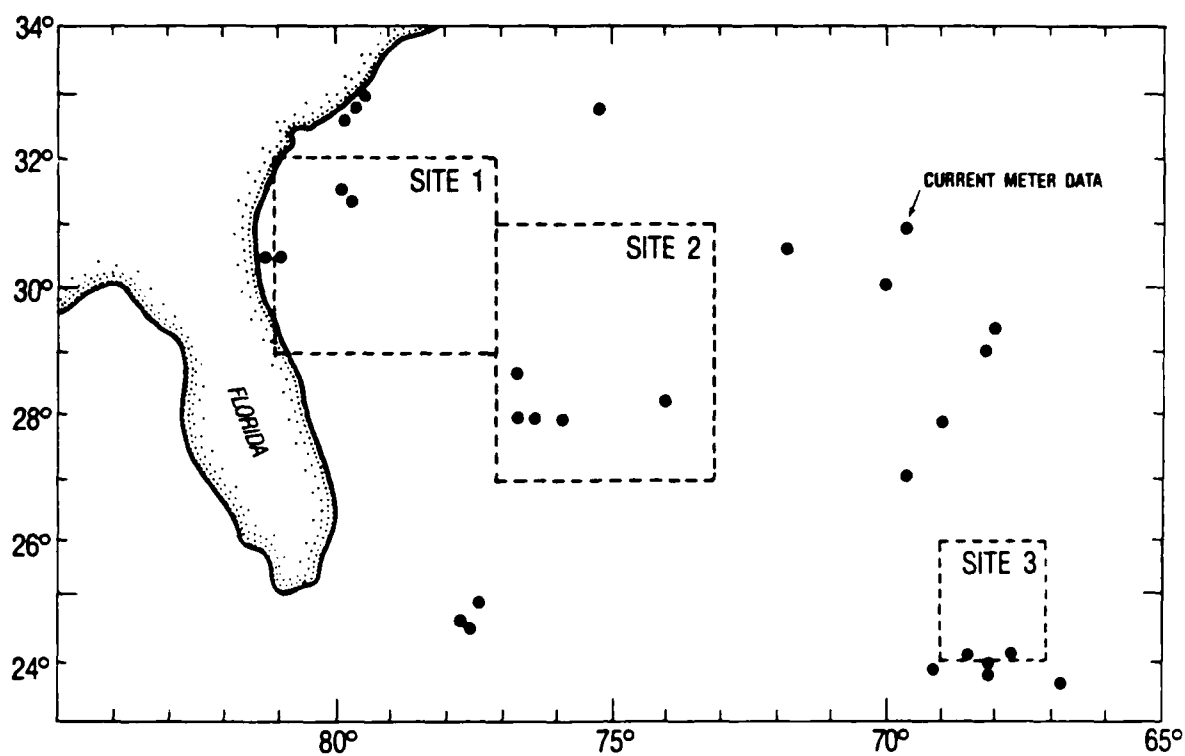


Figure 20. Locations where current meter data were obtained.

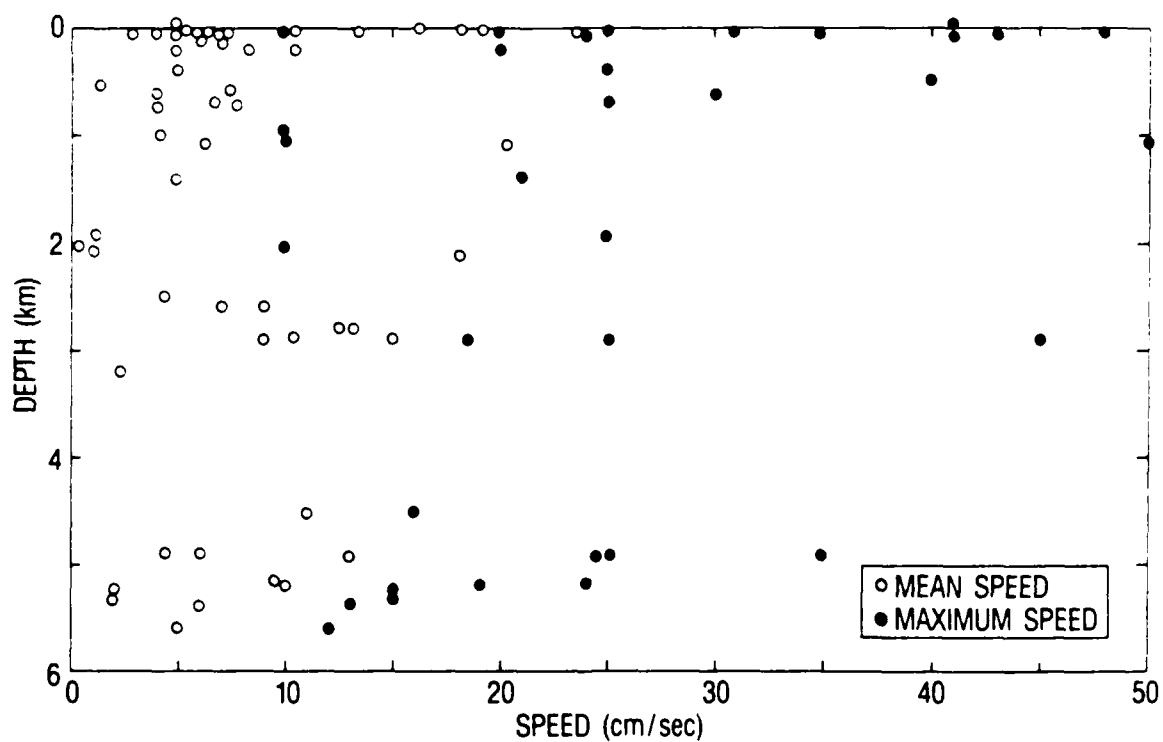


Figure 21. Plot of the mean and maximum current speeds vs. depth for the data obtained at the stations located in Figure 20.

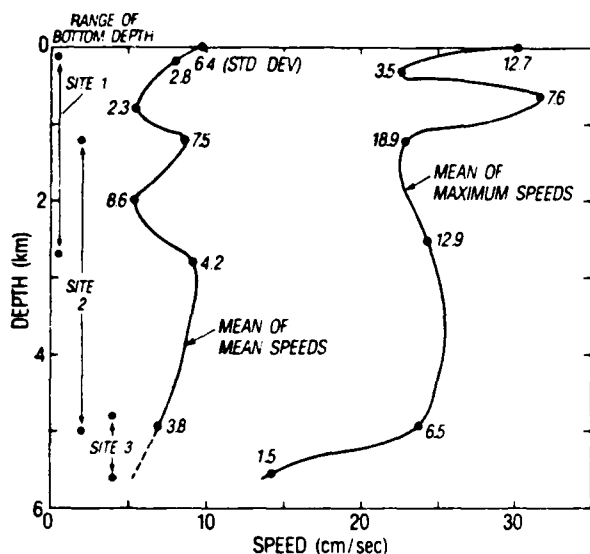


Figure 22. Profiles of the mean values of mean current speeds and maximum current speeds measured at the locations shown in Figure 20 and plotted in Figure 21.

making it the best environment for ocean bottom seismometers, followed by area 2 as second choice and area 1 as the third choice.

VIII. Geoacoustic Models

A. Area I: Seismic Models

Three seismic models are presented for site 534. Because physical properties measurements were not made on the upper 545 m of sediment from hole 534A, the velocity/density values from site 391 were used in constructing the upper 545 m of the models.

The first model (Figs. 23 and 24) was developed by Shipley (1983) to generate synthetic seismograms. He extracted information from the site geophysical logs that are, according to Sheridan (1983b), incomplete and erroneous. Therefore, Shipley also used available common-depth-point (CDP) and sonobuoy data in an attempt to lessen uncertainties about the relative locations of the hole and the seismic sections, the velocity corrections, and the composition of the sediments not recovered in the cores. Figure 25 shows that his model does not produce an exact fit to observed reflections.

The second model (Figs. 26 and 27), which we proposed for this area, is a combination of Shipley's Model 1 to 545 m depth and a manually smoothed version of the laboratory measurements of physical properties from hole 534A to a depth of 1665 m.

For the third model (Figs. 28 and 29), we attempted to refine shallow sediment physical properties data using geologic considerations. Corrections were made for laboratory measurements of sediment velocity and density from sites 391 and 534 to in situ values using

DEPTH	Vp	DENSITY	
4971a	1.54		WATER
			sea floor
.0	1.75	1.70	CLAY, SILT
146.9	1.90	2.00	OOZE
203.5	2.00	2.05	
326.0	1.80	2.05	INTRACLASTIC
354.5	2.10	2.10	MARLY CHALK
500.0	2.00	2.05	
545.8	1.96	1.96	INTERBEDDED
566.6	2.05	1.99	MUDSTONE//CHALK
595.2	2.21	2.06	
660.0	2.72	2.35	CHALK WITH LIMESTONE,
696.5	2.42	2.35	MUDSTONE
714.5	1.90	2.10	
723.5	2.63	2.20	
764.5	1.87	2.10	CLAYSTONE
887.0	1.90	2.07	
914.0	1.77	1.98	
950.0	2.41	2.23	CHALK
976.0	3.38	2.42	INTERBEDDED CHALK,
1044.5	2.28	2.24	CLAYSTONE, LIMESTONE
1107.5	2.83	2.34	
1202.0	3.22	2.46	CHALK WITH LIMESTONE,
1268.0	4.00	2.60	CLAYSTONE
1342.0	3.27	2.45	LIMESTONE
1395.5	2.44	2.33	
1429.0	3.89	2.54	LIMESTONE WITH
1495.6	2.86	2.40	CLAYSTONE
1549.8	3.61	2.48	
1572.0	3.17	2.49	
1617.1	2.73	2.39x	CLAYSTONE
1625.3	2.48	2.41x	
1635.3	5.18	2.73x	BASALT

FOOTNOTE:

x — the compressional velocity and density did not fit any of the published curves. In the case of the claystone (depth = 1625.3 m) the core description mentions the presence of pyrite which might account for the unusually high densities in that section.

Figure 23. Shipley's geoacoustic model 1 for DSDP site 534 (adapted from Shipley, 1983).

the porosity rebound calculations of Hamilton (1975). Below 865 m the model is the same as our second model.

Shipley (1983) attempted the same using the relationships of Hamilton (1975) and the relationships between porosity and vertical velocity from hole 534. Comparison of logging results with corrected values showed that the Hamilton data were adequate for predicting velocity/density changes due to rebound at this site. For the data from hole 534, Shipley felt that there was no systematic rebound for terrigenous sediments below 940 m and for chalks below 700 m. The difference between laboratory and calculated velocities is less than 0.1 km/sec for muds to a depth of 700 m and does not change significantly below that depth. For chalks, the difference is about 0.2 km/sec at depths from 500 to 700 m.

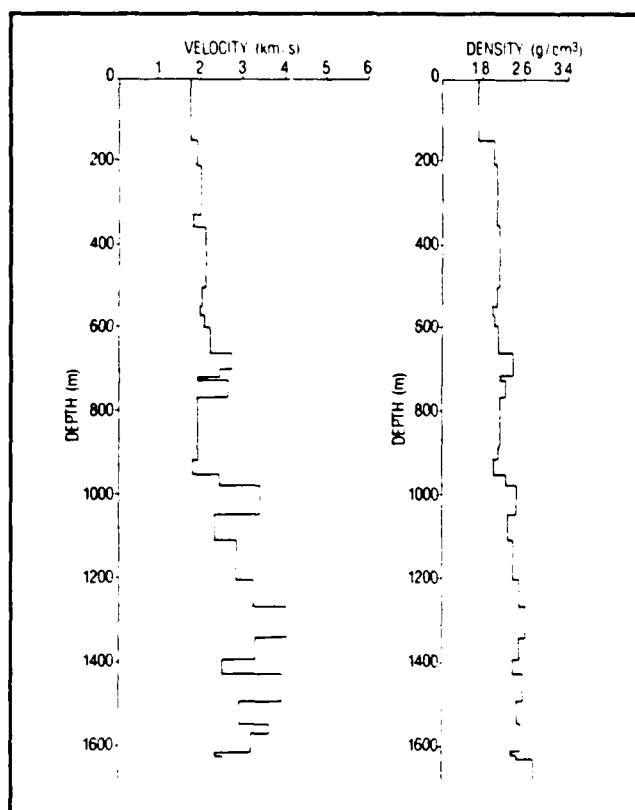


Figure 24. Velocity and density as functions of depth for the Shipley geoaoustic model.

Our seismic models (Figs. 26 and 28) are consistent with Shipley's model and make about the same adjustment for rebound; however, our models include some (observed) high-velocity stringers to retain as much agreement with the "real world" as is practical for geoaoustic modeling. All assumptions, equations, and calculations used to create the models are presented and discussed in the footnotes to the models.

No shear velocity measurements were made at the sites. The shear velocities for the unconsolidated sediments in the models were calculated from compressional velocities using the empirically derived equations of Hamilton (1980). Furthermore, the values used to generate these equations were not measured from calcareous oozes or pelagic clays. Hamilton (1980) stated, however, "in the absence of sufficient data, the same equations are recommended for use in predicting shear wave velocities in calcareous ooze and pelagic clay." At depths over 600 m where we considered the sediments sufficiently compacted, we used a conversion factor of 0.577 (Telford et al., 1976).

Shipley (1983) examined all the seismic lines closest to the site to determine the reflection two-way travel time at the site. He presented the maximum and minimum travel times for these seismic records and the mean value of the three points closest to the site. The travel time for our models falls within the range determined by Shipley.

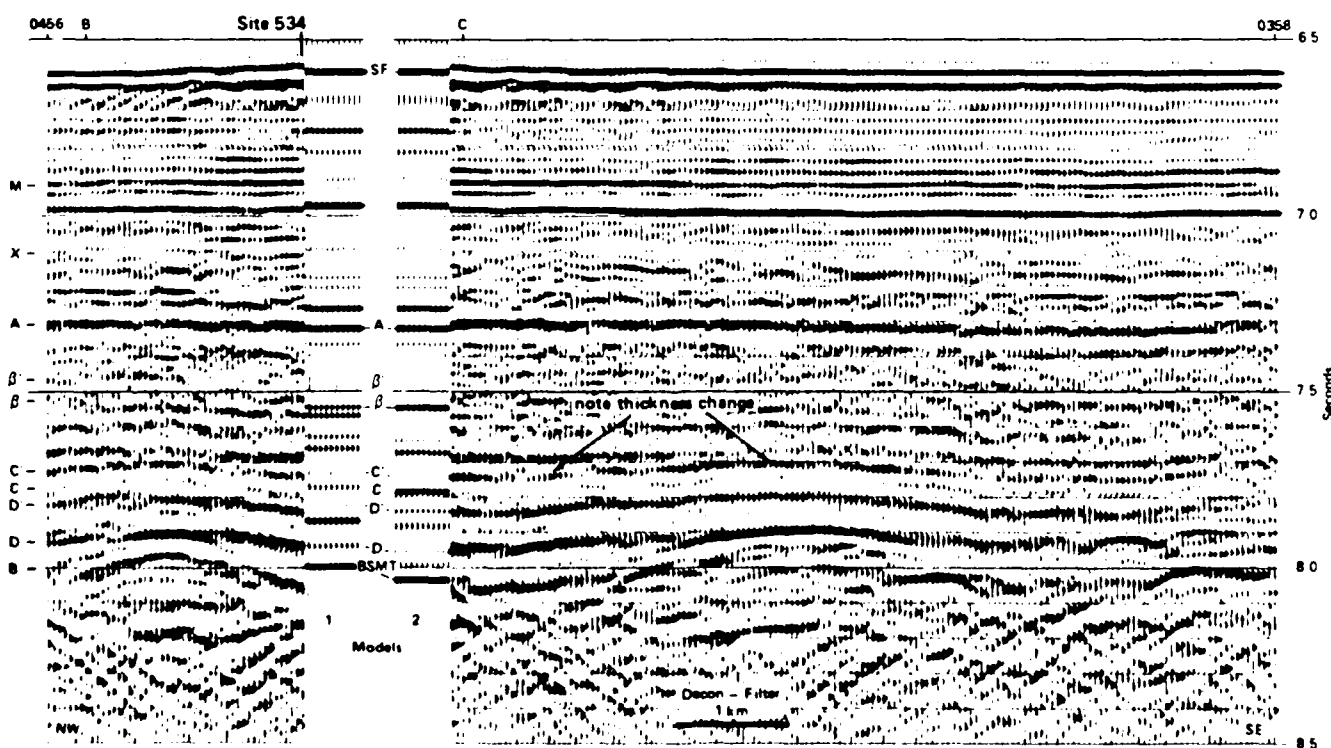


Figure 25. Comparison of the synthetic seismograms generated using Shipley's models 1 and 2 with multichannel records from the site 534 area.

DEPTH	Vp	DENSITY	Vs
.0	1.75	1.70	0.44
147.	1.90	2.00	0.53
204.	2.00	2.05	0.60
326.	1.80	2.05	0.47
355.	2.10	2.10	0.68
500.	2.00	2.05	0.60
548.	1.87	1.70	0.51
600.	4.00	2.50	2.30
623.	2.10	1.80	1.21
646.	4.10	2.50	2.37
660.	2.60	2.20	1.37
708.	2.00	1.70	0.60
732.	4.87	2.00	2.81
737.	1.80		1.04
862.	5.00	2.80	2.89
865.	2.00	2.10	0.60
925.	3.70	2.40	2.14
960.	2.70		1.42
979.	5.00		2.89
995.	4.10		2.37
1030.	4.90	2.65	2.83
1050.	3.20		1.68
1064.	2.05	2.10	0.64
1092.	3.60	2.50	2.08
1111.	3.20		1.85
1140.	4.00		2.31
1160.	3.00		1.58
1236.	4.00		2.31
1308.	3.20		1.85
1330.	3.95		2.28
1400.	2.80		1.47
1429.	5.00		2.89
1468.	2.80	2.70	1.47
1505.	4.00		2.31
1523.	2.42		1.27
1550.	5.00	2.60	2.89
1570.	3.80		2.19
1595.	2.80		1.47
1640.	5.30	2.85	3.06
1655.	5.87		3.39

For Vp from 1.512 to 2.15 k/s the following equations from Hamilton (1980) were used to calculate Vs:

for Vp = 1.512 to 1.555 k/s:
 $V_s = 3.884V_p - 5.757$

for Vp = 1.555 to 1.650 k/s:
 $V_s = 1.137V_p - 1.485$

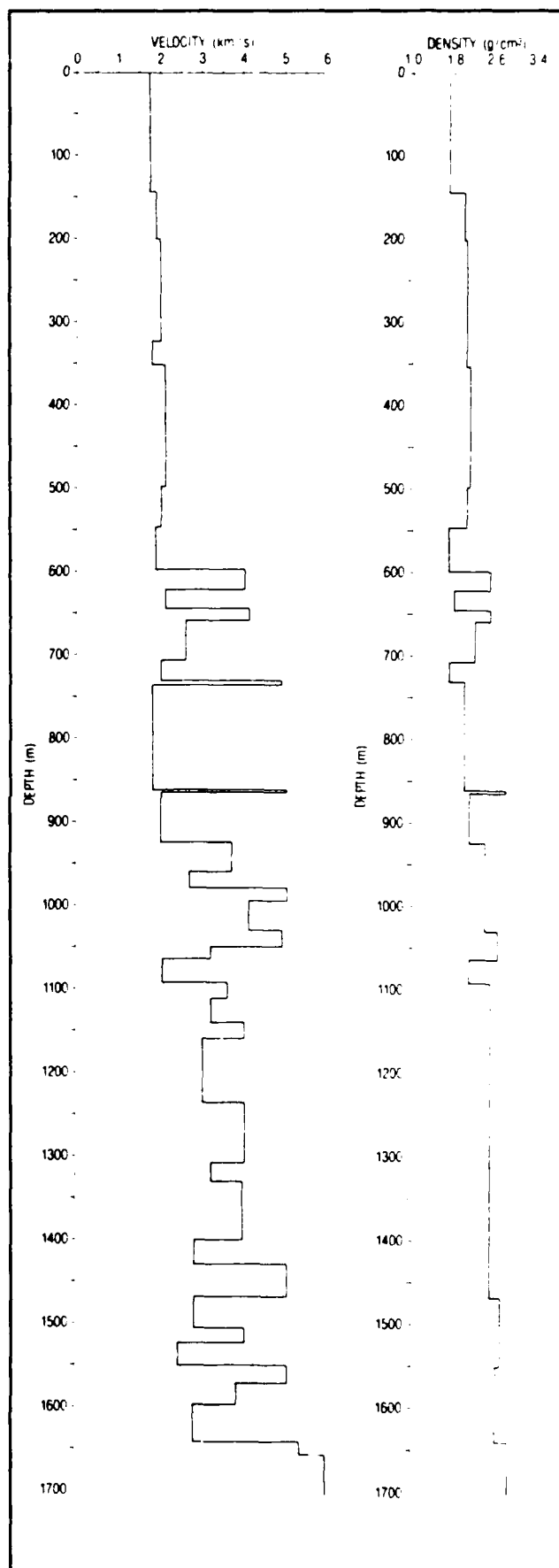
for Vp = 1.650 to 2.150 k/s:
 $V_s = 0.991 - 1.136V_p + 0.47V_p^2$

For Vp from 2.15 to 3.4 k/s the ratio $V_p/V_s = 1.9$ was used where the rock was limestone or chalk (Hamilton, 1980), and also for the two claystones found at depths of 1523 meters and 1595 meters. For other lithologies the Milholland et al. (1980) curves were used.

For Vp greater than 3.4 the ratio of $V_s = .577V_p$ was used (Telford et al., 1976).

Figure 26 (above). Proposed geoaoustic model for site 534. To 545 m depth, this model duplicates Shipley's model 1. Below 545 m, the model was constructed by manually smoothing the shipboard laboratory measurements of sediment velocity and density.

Figure 27 (right). Velocity and density as functions of depth for the proposed geoaoustic model presented in Figure 26.



B. Area II: Seismic Model

In all, six reflectors were recognized on the seismic reflection records from the vicinity of sites 417 and 418. To make the generalized geoaoustic model (Fig. 30), data from site 417 were used. The travel times to all reflectors and the depth to reflector 3, which were determined by the shipboard scientific party (Donnelly et al., 1980), were used as a starting point. As shown, definitive seismic/stratigraphic correlations at this site were not determined. The approximate depths to

reflectors 1, 2, 4, 5, and 6 were calculated using travel times from seismic reflection data (Donnelly et al., 1980). Physical properties measurements on DSDP cores provided information on approximate velocities and depths to sections of the cores with high acoustic impedance contrasts.

We divided the geoaoustic model into 11 layers based on lithology and seismic velocities reported for site 417 (Donnelly et al., 1980). Values presented in the geoaoustic model were determined using several

DEPTH (1)	Vp	Vs (2)	DENSITY (3)	POROSITY (4)	
4971a	1.54				WATER
			sea floor		
.00	1.50b	0.12	1.42	78.	OOZE, CLAY
2.3	1.50b	0.12	1.43	77.6	
4.9	1.51b	0.12		93.6	
8.0	1.51b	0.12		88.4	SILTY CLAY, CALCAREOUS OOZE
88.6	1.58b	0.31	1.44		
94.3	1.59b	0.32	1.76z	48.0	
146.9	1.90b	0.53	2.00		INTRACLASTIC MARLY CHALK
203.5	2.00	0.60	2.05		
326.0	1.80	0.47	2.05		
354.5	2.10	0.68	1.91z	49.4	
474.6	2.00	0.60	2.05z	43.3	
500.0	2.00	0.60		44.0	INTERBEDDED MUDSTONE/CHALK
548.	1.92	0.54	1.90		
600.	4.00	2.11	2.50	14.	CHALK WITH LIMESTONE, MUDSTONE
623.	2.15	0.78m	1.91z	45.	
646.	4.10	2.37	2.50	12.	
660.	2.60	1.20n	2.20z	24.	
708.	2.05	0.60	1.81z	40.	CLAYSTONE
732.	4.87	2.65n		12.	
737.	1.97	0.58	2.15z	43.	
862.	5.00	x	2.80	5.	
865.	2.24	0.75m	2.20z	43.	
925.	3.70	1.95	2.40	30.	CHALK
963.	2.70	1.56c	2.32	26.	
979.	5.00	2.89c		3.	INTERBEDDED CHALK, CLAYSTONE, LIMESTONE
995.	4.10	2.37c	2.40	10.	
1030.	4.90	x	2.65	9.	
1050.	3.20	1.85c	2.30	16.	
1064.	2.05	1.18c	2.10	36.	
1092.	3.60	2.08c	2.50	15.	
1111.	3.20	1.85c	2.30	36.	
1140.	4.00	2.30c	2.30	13.	
1160.	3.00	1.73c	2.30	20.	CHALK WITH LIMESTONE, CLAYSTONE
1236.	3.40	1.96c	2.30	20.	
1280.	4.00	2.30c	2.30	15.	
1308.	3.20	1.85c	2.30	21.	LIMESTONE
1330.	3.95	2.28c	2.30	18.	
1390.	2.80	1.62c	2.30	25.	LIMESTONE WITH CLAYSTONE
1429.	5.00	x	2.70	5.	
1468.	2.80	1.62c	2.3	24.	
1505.	4.00		2.7	8.	
1523.	2.42	1.40c	2.36	24.	CLAYSTONE
1550.	5.00	x	2.60	5.	
1570.	3.80	2.19c	2.60	12.	
1595.	2.80		2.60	22.	
1640.	5.30	2.75	2.65	13.	BASALT
1654.0	5.87	3.09	2.82	9.	

Figure 28. Second geoaoustic model for site 534. This model is a refinement of the model shown in Figure 26. It corrects the laboratory-measured sediment velocity and density values to in situ values.

LEGEND — FIGURE 28

(1) Water depth is water column thickness; sediment depth is depth below sea floor.

(2) V_s was calculated using the following equations of Hamilton (1980) for sediments to a depth of 600 meters.

$$\text{for } V_p = 1.512 \text{ to } V_p = 1.555 \text{ k/s: } V_s = 3.884V_p - 5.757$$

$$\text{for } V_p = 1.555 \text{ to } V_p = 1.650 \text{ k/s: } V_s = 1.137V_p - 1.485$$

$$\text{for } V_p = 1.650 \text{ to } V_p = 2.150 \text{ k/s: } V_s = 0.991 - 1.136V_p + 0.47V_p^2$$

$$\text{for } V_p \text{ greater than } 2.150 \text{ k/s: } V_s = 0.78V_p - 0.962$$

Shear velocities without notation were obtained using the equations above, or, the relationship

$$V_p = 1.9V_s$$

where the lithology and the compressional velocity and density indicated the layer was composed of limestone or similar rock (from Hamilton, 1980).

V_s for the sediment surface was calculated using a 13:1 ratio for $V_p:V_s$ (Hamilton, 1980).

For basalt the velocity-density curves of Christensen and Salisbury (1975) were used.

Shear velocities with notation were obtained using the methods described in part 2 below.

(3) Density is wet bulk density. A density of 1.49 gm/cc was measured at 2.3 meters in the core. An expected value would be about 1.44 gm/cc (Hamilton, 1975; Tucholke and Shirley, 1980). Assuming a grain density of 2.73 gm/cc, a water density of 1.05 gm/cc, and a porosity of 78% we calculated the density at the sediment surface to be 1.42 gm/cc. This value is much closer to the normal values for abyssal plain sediments.

At depths of less than 90 meters density changes in oozes due to compaction rebound in cores is negligible (Hamilton, 1975). Where densities were taken directly from the Shipley model no adjustments were made. For non-lithified sediments between 600 and 900 meters densities indicated by notation (z) were corrected as explained in part 2 below.

(4) Porosity above 500 meters is shipboard measured value at that depth; below 500 meters where the range of values was greater it is an approximate mean for the values from that depth to the next.

a - Water velocity taken from NORDA database (J. Soileau, pers. comm.)

b - V_p at the water sediment interface is indicated at a depth of .0 meters. Shipboard measured V_p at 2.28 meters was 1.47 k/s, giving a low V_o/V_w ratio of .95. In situ corrections, calculated according to Hamilton (1971), would increase the compressional velocity by about .013 k/s. The work of Tucholke and Shirley (1979) comparing in situ with laboratory "in situ corrected" velocities suggests that the corrected laboratory velocities should be between .01 and .02 k/s slower than the in situ values. Therefore, the compressional velocity at the sea floor is estimated to be 1.50 k/s. The V_o/V_w ratio is then .97 which is consistent with the ratios calculated by Tucholke and Shirley (1979) in the Nares Abyssal Plain. For this model the shipboard measured velocities from the sediment surface to 8.0 meters also have been increased by .03 k/s.

In order to make the velocities closer to the interval velocity of 1.75 k/s for the first layer of Shipley's model (1983) the compressional velocities at depths from 8 to 94.6 meters were increased by .07 k/s. The model between 146.9 and 500.0 meters is taken directly from Shipley (1983). In situ corrections for velocities at depths between 548 and 925 meters were based on the compaction rebound calculations of Hamilton (1975) and the velocity/density curves for hole 534 plotted in Shipley (1983).

c - V_s was obtained by using the relationship $V_s = .577 V_p$.

m - V_s was obtained using the velocity-density curves of Millholland et al (1980).

n - V_s was obtained using the velocity-density curves of Nafe and Drake (Ludwig et al., 1970).

x - The density is unusually high for this velocity and does not fall on or near any of the empirical curves. The high density is probably the result of a measuring error. No V_s was calculated; using the V_p/V_s ratio of Hamilton (1980) the shear velocity for a limestone with a compressional velocity of 5.0 km/sec would be 2.63 km/sec. If the densities are correct, the data for anhydrite, which is characterized by high densities and low velocities, might be used to estimate a value.

z - Correction for compaction rebound was made using the following relationship:

$$D_{ins} = (P_{ins} \times D_w) + \frac{(1-D_{ins})(D_{wb}-P_1 \times D_w)}{(1-P_1)}$$

where D_{ins} = in situ density

D_w = pore water density

D_{wb} = wet bulk density

P_{ins} = in situ porosity

P_1 = laboratory measured porosity

The value chosen for pore water density, provided it is reasonable for the area, has a negligible effect on the calculation of in situ density value. Pore water density used was 1.03.

different sources. The footnotes to Figure 30 indicate how a given value was obtained.

C. Area III: Seismic Model

The velocity profile presented in Figure 31 indicates the number and types of layers and their approximate seismic velocities, which might typify the Blake Plateau. The data used for the model were taken from the reports of DSDP drill hole 389, the multichannel seismic reflection study by Shipley et al. (1978), and the multichannel seismic reflection study by Sheridan et al. (1981). Only compressional velocities are presented, and no attempt has been made to correct laboratory values to in situ values.

D. Area IV: Velocity Profiles

The plots of velocity vs. depth presented in Figure 32 are examples of what might be expected in the Straits of Florida and Northeast Providence Channel (Fig. 1). The data used for these models are multichannel seismic reflection velocity values from Sheridan et al. (1981). On the Bahama Banks the nature and thickness of the carbonate deposits are highly variable; therefore, it is not possible to create a single model that will be representative of the whole area.

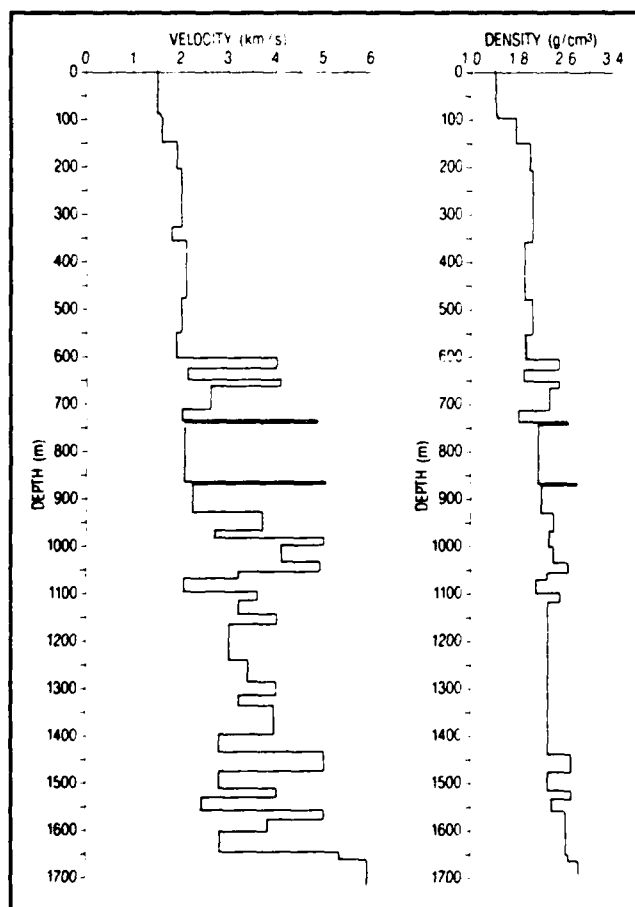


Figure 29. Velocity and density as functions of depth for the model shown in Figure 28.

E. Area V: Seismic Model

Figure 18 shows a correlation of seismic reflectors with lithologic units at DSDP site 387, located west of Bermuda (Tucholke et al., 1979). Also presented in Figure 18 is a seismic velocity model based on calculated interval velocities determined from these lithologic correlations and the seismic travel times to the reflectors. We used this site as representative of geologic conditions on the Bermuda Rise rather than site 386, where Eocene-Oligocene volcanoclastic turbidites were encountered. Because these turbidites encircle Bermuda and are a local phenomenon, site 386 is less typical of the Bermuda Rise. We have, however, included data from site 386 (Appendices A-3 and A-4) so that the physical properties measurements for these turbidites are available if needed.

IX. Summary and Conclusions

For an accurate geoacoustic model to be constructed the geology of the area must be well understood. In some areas modeling may not be successful because small-scale lithologic and topographic changes are not recognized from the available data. Currently, we do not have the ability to obtain complete measurements of such sediment properties as velocity and density from a drill hole. Laboratory and in situ measurements do not agree, and attempts to reconcile the two have not been completely effective. In constructing our geoacoustic models we have tried to build on the work of others, most notably, the empirically derived equations of Hamilton (1980, 1975, 1971) and seismic studies at the DSDP sites. In our models, we have added high-velocity stringers which are almost always present in nature; for example, worldwide occurrences of chert have been documented by DSDP cores.

We have chosen five areas of the western North Atlantic Ocean and constructed geoacoustic models for each area. For two areas we used the laboratory and seismic data collected during DSDP studies, as well as published reports, to construct detailed models. For the remaining three areas we have tabulated generalized sediment velocity and lithology information from published reports.

Using data from DSDP site 534, Shipley (1983) constructed two models from which he generated synthetic seismograms. Our proposed model for site 534 uses a constant interval velocity of 1.75 km/sec for the top 147 m of sediment and 1.9 km/sec for the next 57 m in accordance with Shipley's model. The Shipley model was also used between 204 m and 545 m depth. Velocities at these depths are variable and range between 1.8 km/sec and 2.1 km/sec. The remainder of our first model was obtained by smoothing the velocities measured from core samples. Our second site 534 model is similar to the first except for the upper 147 m

LAYER	COMPOSITION	DEPTH ¹ (m)	VELOCITY (km/sec) Vp Vs		DENSITY	POROSITY
	WATER ²	5482	1.553		1.05	
1 REFLECTOR 1	CLAY	0.8 61 ^a	1.51 ^c $\bar{v} \approx 1.50$	0.10 ^d 0.10 ^d	1.51 $\bar{p} = 1.6$	71.9
2 REFLECTOR 2	CLAY	139 ^a	$\bar{v} \approx 1.53$	0.26 ^d	1.65	
3 REFLECTOR 3	SILTY CLAY	156 ^b	$\bar{v} \approx 1.61$	0.35 ^d	1.75	71.1
4 REFLECTOR 4	CLAY	213 ^a	$\bar{v} \approx 1.63$	0.40 ^d	1.75	59.0
5 REFLECTOR 5	SANDY CLAY, CLAYSTONE, CHALK, SAND,	260 ^a 278	$\bar{v} \approx 1.67$		1.95	
6 REFLECTOR 6	CHERT	298 ^a	2.06	0.95 ^e	1.82	53.9
7	SAND, MARL, CLAYSTONE,	327	$\bar{v} \approx 1.77$			
8	CHERT, SOME CHALK	333	2.25		2.25	38.8
9 BASEMENT REFLECTOR		343	1.85	0.95 ^f	2.06	48.8
10	BASALT	415	5.34	2.69 ^g	2.78	8
11			5.65	2.88 ^g	2.82	5

Figure 30. Geoacoustic model for sites 417 and 418. Velocities were determined as explained in the footnotes: (1) Depth where it applies to water means water column thickness; for sediments, depth indicates distance below the water/sediment interface. (2) Water depth: corrected echo sounding value at site 417D; velocity: NORDA data base (J. Soileau, NORDA pers. comm.) and Tucholke and Shirley (1979) (both values were in agreement). (a) Calculated for this report using the velocities indicated in the Vp column. (b) Calculated by DSDP scientific party using seismic reflection data. (c) Approximated using the "laboratory corrected to in situ" values obtained by Tucholke and Shirley (1979) for cores in the Nares Abyssal Plain. (d) Calculated using the equations from Hamilton (1980): for Vp from 1.512 to 1.555 km/sec, Vs = 3.884Vp - 5.757; for Vp from 1.555 to 1.650 km/sec, Vs = 1.137Vp - 1.485. (e) Determined from Vp/Vs relationships of Milholland et al. (1980). (f) Density indicates that the sediments are well indurated, so the Vp = 1.9Vs relationship of Hamilton was used. (g) From Christensen and Salisbury (1975).

LAYER	DEPTH	VELOCITY	COMPOSITION
1	0.0		Mn nodules, foram sand
2	0.1	1.52	nannofossil ooze
3	47	1.55	ooze
4	95	1.63	marly ooze
5	110	1.60	nannofossil ooze
6	140	1.71	marly nannofossil ooze
7	160	1.8	chalk, interbedded limestone
8	300	2.6	limestone
9	600	3.4	limestone
10	2000	4.4	limestone
11	3000	5.0	limestone
12	6000	5.7	limestone
13	8000	6.1	volcaniclastics
14	11000	6.7	transitional crust

Figure 31. Generalized geoacoustic model for the Blake Plateau. Laboratory measurements from site 389 were used for the first 300 m of sediment; the remainder of the model is based on multichannel seismic reflection data from Shipley et al. (1978) and Sheridan et al. (1981).

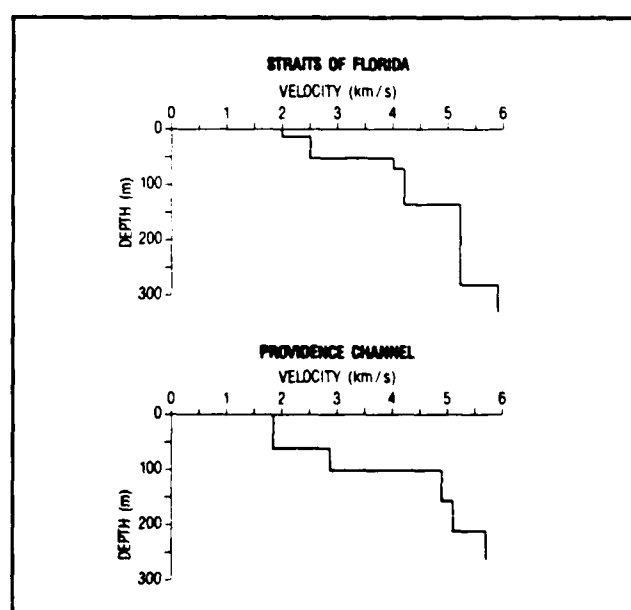


Figure 32. Generalized plots of velocity as a function of depth for the N.E. Providence Channel and the Straits of Florida based on published multichannel seismic reflection data (Sheridan et al., 1981).

of sediment where laboratory-measured velocities were corrected to in situ values. From 545 m to 865 m, small adjustments were made to the first model in an attempt to approximate in situ values of velocity and density. Both models contain velocity inversions and high-velocity stringers.

The model for sites 417 and 418 contains 11 layers and was constructed using seismic and physical properties data from the DSDP site 417 and 418 reports. It contains two high-velocity stringers associated with two chert intervals found in the cores.

In working on data from these five sites it became apparent to us that some areas (for example, the Bahama Banks) have such rugged topography and such variable lithology that traditional modeling attempts probably will be unsuccessful unless the geology is known in great detail. Some continental margin shallow-water sites and some deep ocean sites, such as DSDP site 417/418, are much more predictable and should be easier to model; however, even site 417/418 has unique geologic factors that will cause actual seismic propagation to differ from our model predictions. However, deviations from predicted values should be reasonably small at low (5-50 Hz) frequencies.

X. References

- Amos, A. F., A. L. Gordon., and E. D. Schneider (1971). Water masses and circulation patterns in the region of the Blake-Bahama Outer Ridge. *Deep-Sea Research* 18: 145-165.
- Benson, W. E., R. E. Sheridan, et al. (1978). Site 391: Blake-Bahama Basin. *Initial Reports of the Deep-Sea Drilling Project*, Washington, U.S. Govt. Printing Office, v. 44, pp. 153-336.
- Bowles, F. A. (1980). Stratigraphy and sedimentation of the archipelagic apron and adjoining area south-east of Bermuda. *Marine Geology* 37: 267-294.
- Boyd, J. D. (1984). Currents near Deep-Sea Drilling Project Hole 395A and Effects on Components of the Marine Seismic System Project. In *Initial Reports of the Deep-Sea Drilling Project*, Washington, U.S. Govt. Printing Office, v. 78, pp. 759-766.
- Bryan, G. M., R. G. Markl, and R. E. Sheridan (1980). IPOD Site Surveys in the Blake-Bahama Basin. *Marine Geology* 35: 43-63.
- Childs, O. E. (1985). Correlation of stratigraphic units of North America. *American Association of Petroleum Geologists Bulletin* 69(2): 181-189.
- Christensen, N. I. and M. H. Salisbury, (1975). Structure and constitution of the lower oceanic crust. *Rev. Geophys. Space Phys.* 13: 57-86.
- Detrick, R. E. and G. M. Purdy, (1980). The crustal structure of the Kane Fracture Zone from seismic refraction studies. *Journal of Geophysical Research* 85: 3759-3778.
- Dillon, W. P., C. K. Paull, R. T. Buffler, and J-P. Fail (1979). Structure and development of the Southeast Georgia Embayment and Northern Blake Plateau: Preliminary analysis. In *Geologic and Geophysical Investigations of Continental Margins*; J. S. Watkins, L. Montadert, and P. W. Dickerson, (eds.), AAPG Memoir 29: 27-41.
- Dillon, W. P., J. A. Grow and C. K. Paull (1980). Unconventional gas hydrate seals may trap gas off southeast U.S. *Oil & Gas J.* 78(1): 124-130.
- Dillon, W. P., P. Popenoe, J. A. Grow, K. D. Klitgord, B. A. Swift, C. K. Paull, and K. V. Cashman (1982). Growth faulting and salt diapirism: Their relationship and control in the Carolina Trough, Eastern North America. *AAPG Memoir* 34: 21-46.
- Donnelly, T., J. Francheteau, W. Bryan, P. Robinson, M. Flower, M. Salisbury, et al. (1980). *Initial Reports of the Deep-Sea Drilling Project*, v. 51, 52, and 53. Washington, U.S. Govt. Printing Office.
- Duennebie, F. K., G. Blackinton, and G. H. Sutton (1981). Current generated noise recorded on ocean bottom seismometers. *Marine Geophysical Researches* 5: 109-115.
- Ewing, J. I. and M. Ewing (1962). Reflection profiling in and around the Puerto Rico Trench. *Journal of Geophysical Research* 67: 4729-4739.
- Ewing, J. I., C. C. Windisch, and M. Ewing (1970). Correlation of Horizon A with JOIDES borehole results. *Journal of Geophysical Research* 75: 5645-5653.
- Ewing, M. and J. I. Ewing (1963). Sediments at proposed LOCO drilling sites. *Journal of Geophysical Research* 68: 251-256.
- Grow, J. A. and R. G. Markl (1977). IPOD-USGS seismic reflection profile from Cape Hatteras to the Mid-Atlantic Ridge. *Geology* 5: 625-630.
- Hamilton, E. L. (1980). Geoacoustic modeling of the sea floor. *Journal of the Acoustical Society of America* 68(5): 1313-1340.
- Hamilton, E. L. (1975). *Acoustic and Related Properties of the Sea Floor: Density and Porosity Profiles and Gradients*. Naval Undersea Center Technical Report.
- Hamilton, E. L. (1971). Prediction of in-situ acoustic and elastic properties of marine sediments. *Geophysics* 36(2): 266-284.
- Hogg, N. G. (1983). A note on the deep circulation of the western North Atlantic: Its nature and causes. *Deep-Sea Research* 30(A): 945-961.
- Jansa, L. F., P. Enos, B. E. Tucholke, F. M. Gradstein, and R. E. Sheridan (1979). Mesozoic-Cenozoic sedimentary formations of the North Atlantic Basin; Western North Atlantic. In *Deep Drilling Results in the Atlantic Ocean, Continental Margins and Paleo Environments*, M. Talwani,

W. Hay, and W. F. B. Ryan (eds.), American Geophysical Union, Maurice Ewing Series, v. 3 pp. 1-57.

Kelley, E. A. and G. L. Weatherly (1985). Abyssal eddies near the Gulf Stream. *Journal of Geophysical Research* 90(C2): 3151-3159.

Klitgord, K. D. and J. C. Behrendt (1979). Basin structure of the U.S. Atlantic Margin. *American Association of Petroleum Geologists*, Memoir 29: 89-112.

Klitgord, K. D. and J. A. Grow (1980). Jurassic seismic stratigraphy and basement structure of the western Atlantic magnetic quiet zone. *American Association of Petroleum Geologists Bulletin* 64: 1658-1680.

Klitgord, K. D., P. Popenoe, and H. Schouten (1984). Florida: A Jurassic transform plate boundary. *Journal of Geophysical Research* 89(B9): 7753-7772.

Lai, D. Y. (1984). Mean flow and variabilities in the deep western boundary current. *Journal of Physical Oceanography* 14(9): 1488-1498.

Laine, E. P. (1978). *Geologic Effects of the Gulf Stream System in the North American Basin*. MIT-WHOI Joint Program, Ph.D. Thesis, pp. 164.

Li, L., M. Wimbush, D. R. Watts, A. J. Brincko, and T. N. Lee (1985). Gulf Stream and wind-induced current variability on the Georgia Continental Shelf, Winter 1978. *Journal of Geophysical Research* 90(C2): 3199-3210.

Lowrie, A., Jr. and B. C. Heezen (1967). Knoll and sediment drift near Hudson Canyon. *Science* 157: 1552-1553.

Ludwig, W. J., J. E. Nafe, and C. L. Drake (1970). Seismic refraction. In *The Sea*, v. 4, Part 1, A. E. Maxwell (ed.), Wiley, New York, pp. 53-84.

Markl, R. G., G. M. Bryan, and J. I. Ewing (1970). Structure of the Blake-Bahama Outer Ridge. *Journal of Geophysical Research* 75: 4539-4555.

Markl, R. G. and G. M. Bryan (1983). Stratigraphic evolution of Blake Outer Ridge. *American Association of Petroleum Geologists Bulletin* 67(4): 666-683.

Milholland, P., M. H. Manghani, S. O. Schlanger, and G. H. Sutton (1980). Geoacoustic modeling of deep-sea carbonate sediments. *Journal of the Acoustical Society of America* 68(5): 1351-1360.

Mills, C. A., S. A. Tarbell, and R. E. Payne (1981). *A Compilation of Moored Instrument Data and Associated Hydrographic Observations, Vol. XXVII (Polymode Local Dynamics Experiment, 1978-1979)*. Woods Hole Oceanographic Institution, Woods Hole, Massachusetts, Tech. Rept. WHOI 81-73.

Mutter, J. C. and R. E. Detrick (1984). Multichannel seismic evidence for anomalously thin crust at Blake Spur Fracture Zone. *Geology* 12: 534-537.

Nafe, J. E. and C. L. Drake (1963). Physical properties of marine sediments. In *The Sea*, v. 3, A. E. Maxwell (ed.), Wiley, New York, pp. 794-815.

NAVOCEANO (1964-1982). Unpublished data reports on moored current meter arrays. Naval Oceanographic Office, Stennis Space Center, Mississippi.

NAVOCEANO (1965). *Oceanographic Atlas of the North Atlantic Ocean, Section V, Marine Geology*. Naval Oceanographic Office, Stennis Space Center, Mississippi, Pub. No. 700.

Neumann, G. and W. J. Pierson, Jr. (1966). *Principles of Physical Oceanography*. Prentice Hall, Inc., Englewood Cliffs, New Jersey, 545 p.

Paull, C. K. and W. P. Dillon (1981). *Appearance and Distribution of Gas Hydrate Reflection in the Blake Ridge Region, Offshore Southeastern United States*. USGS Miscellaneous Field Studies Map MF-1252.

Paulus, F. J. (1972). The geology of site 98 and the Bahamas Platform. In *Initial Reports of the Deep-Sea Drilling Project* v. 11, Washington, U.S. Govt. Printing Office, pp. 877-897.

Perkins, H. and M. Wimbush (1976). A cyclonic mini-eddy near the Blake Escarpment. *Geophysical Research Letters* 3(10): 625-626B.

Perry, R. K., H. S. Fleming, P. R. Vogt, N. Z. Cherkis, R. H. Feden, J. Theide, J. E. Strand, and B. J. Collette (1981). *North Atlantic Ocean, Bathymetry and Plate Tectonic Evolution*. Geological Society of America Map and Chart Series MC-35.

Popenoe, P. (1984). *Summary Geologic Report for the South Atlantic Outer Continental Shelf (OCS) Planning Area* (Supplement to Report 83-186). USGS Open File Report 84-476, p. 12.

Pinet, P. R. and P. Popenoe (1985). Shallow seismic stratigraphy and post-Albian geologic history of the northern and central Blake Plateau. *Geological Society of America Bulletin* 96: 627-638.

Riser, S. C., H. Freeland, and T. H. Rossby (1978). Mesoscale motions near the deep western boundary of the North Atlantic. *Deep-Sea Research* 25: 1179-1191.

Salisbury, M. H., R. Stephen, N. I. Christensen, J. Francheteau, H. Yozo, M. Hobart, and D. Johnson (1980). The physical state of the upper levels of Cretaceous oceanic crust from the results of logging, laboratory studies, and the Oblique Seismic Experiment at Deep Sea Drilling Project, Sites 417 and 418. In *Initial Reports of the Deep-Sea Drilling Project*, v. 51, 52, and 53, Donnelly, T., J. Francheteau, W. Bryan, P. Robinson, M. Flower, M. Salisbury, et al. (eds.), Washington, U.S. Govt. Printing Office, pp. 1579-1597.

Schmitz, W. J., Jr. (1977). On the deep general circulation in the western North Atlantic. *Journal of Marine Research* 35(1): 21-28.

Schouten, H. and K. D. Klitgord (1977). *Map showing Mesozoic magnetic anomalies, western North Atlantic*. USGS Misc. Field Studies Map MF-915.

Sheridan, R. E. (1978). Structural and stratigraphic evolution and petroleum potential of the Blake Plateau. *Proceedings, Offshore Technology Conference*, pp. 363-368.

Sheridan, R. E., L. G. Bates, T. H. Shipley, and J. T. Crosby (1983a). Seismic Stratigraphy in the Blake-Bahama Basin and the Origin of D. Horizon. In *Initial Reports of the Deep-Sea Drilling Project*, v. 76, R. E. Sheridan, F. M. Gradstein, et al. (eds.), Washington, U.S. Govt. Printing Office, pp. 667-683.

Sheridan, R. E., J. T. Crosby, G. M. Bryan, and P. L. Stoffa (1981). Stratigraphy and structure of Southern Blake Plateau, North Florida Straits, and Northern Bahama Platform from multichannel seismic reflection data. *American Association of Petroleum Geologists Bulletin* 65(12): 2571-2593.

Sheridan, R. E., F. M. Gradstein, et al. (1983b). Site 534, Blake-Bahama Basin. In *Initial Reports of the Deep-Sea Drilling Project*, v. 76, Washington, U.S. Govt. Printing Office, pp. 141-340.

Shipley, T. H. (1983). Physical Properties, Synthetic Seismograms, and Seismic Reflections, Correlations at Deep Sea Drilling Site 534, Blake-Bahama Basin. In *Initial Reports of the Deep-Sea Drilling Project*, v. 76, R. E. Sheridan, F. M. Gradstein, et al. (eds.), Washington, U.S. Govt. Printing Office, pp. 653-666.

Stephen, R. A., K. E. Loudon, and D. H. Matthews (1980). The Oblique Seismic Experiment on Deep Sea Drilling Project Leg 52. In *Initial Reports of the Deep-Sea Drilling Project*, v. 51, 52, and 53; T. Donnelly, J. Francheteau, W. Bryan, P. Robinson, M. Flower, M. Salisbury, et al. (eds.), Washington, U.S. Govt. Printing Office.

Sutton, G. J., F. K. Duennebier, B. Iwatake, and J. D. Tuthill (1981b). An overview and general results of the Lopez Island OBS Experiment. *Marine Geophysical Researches* 5: 3-34.

Telford, W. M., L. P. Geldart, R. E. Sheriff, and D. A. Keys (1976). *Applied Geophysics*. Cambridge University Press, Cambridge, England, 860 p.

Tucholke, B. E. (1979). Relationships between acoustic stratigraphy and lithostratigraphy in the western North Atlantic Basin. In *Initial Reports of the Deep-Sea Drilling Project*, v. 43, B. R. Tucholke, P. R. Vogt, et al. (eds.), Washington, U.S. Govt. Printing Office, pp. 827-846.

Tucholke, B. E. and G. S. Mountain (1979). Seismic stratigraphy, lithostratigraphy, and paleosedimentation patterns in the North American Basin. In *Deep Drilling Results in the Atlantic Ocean, Continental Margins and Paleoenvironment*, M. Talwani, W. Hay, and W. B. F. Ryan (eds.), American Geophysical Union, Washington, D. C., pp. 58-86.

Tucholke, B. E. and D. J. Shirley (1979). Comparison of laboratory and in situ compressional wave velocity measurements on sediment cores from the western North Atlantic. *Journal of Geophysical Research* 84(B2): 587-695.

Tucholke, B. E. and P. R. Vogt, et al. (1979). Site 387, Cretaceous to Recent sedimentary evolution of the western Bermuda Rise. In *Initial Reports of the Deep-Sea Drilling Project*, v. 43, Washington, U.S. Govt. Printing Office, pp. 323-391.

Vogt, P. R. (1973). Early events in the opening of the North Atlantic. In *Implications of Continental Drift to the Earth Sciences*, v. 2, D. H. Tarling and S. K. Runcorn (eds.), Academic Press, New York, pp. 693-712.

Webster, F. (1969a). Vertical profiles of horizontal ocean currents. *Deep-Sea Research* 16(1): 85-98.

Webster, F. (1969b). Turbulence spectra in the ocean. *Deep-Sea Research* 16: 357-368.

Webster, F. (1971). On the intensity of horizontal ocean currents. *Deep-Sea Research* 18: 885-893.

Wilcox, J. D. (1978). *A Survey of Current Speed Measurements in the Deep Ocean*. Naval Underwater Systems Center, NUSC Tech. Mem. 781176. Newport, Rhode Island, and New London, Connecticut.

Appendix A-1. Listing of Laboratory-measured Physical Properties for Sediments from DSDP Sites 534 and 391

DSDP SITE 534

<u>DEPTH</u>	<u>Vp</u>	<u>DENSITY</u>
546.8	1.68	1.59
556.9	1.99	2.00
558.1	1.65	1.61
566.5	2.86	2.28
569.1	1.71	1.67
575.1	2.16	2.10
576.7	1.69	1.71
587.2	2.09	2.04
589.5	1.93	1.95
596.3	1.72	1.70
599.3	1.87	2.03
603.1	3.91	2.46
614.5	1.71	1.72
615.5	2.30	2.04
617.2	4.08	2.49
622.6	1.95	2.00
623.2	1.75	1.73
634.5	1.78	1.72
636.3	2.18	2.05
644.6	2.12	1.95
646.3	4.18	2.50
651.3	1.77	1.71
656.3	3.76	2.44
660.2	2.16	2.16
671.8	2.22	2.16
679.3	2.59	2.29
687.2	4.98	2.56
688.9	2.36	2.27
697.9	1.95	1.96
705.6	2.68	2.10
707.5	1.98	1.71
732.5	4.87	2.48
741.6	1.76	2.03
743.1	1.70	2.03
750.8	1.83	2.05
760.5	1.76	2.03
764.9	1.77	2.02
776.8	1.73	1.94
785.6	1.71	1.93
793.6	1.84	1.85
803.8	1.70	1.86
812.3	1.72	1.97
821.5	1.83	2.03

822.2	1.74	1.88
831.5	1.76	2.00
832.8	1.96	2.18
840.8	1.73	1.97
843.3	1.76	2.06
850.1	1.77	2.06
850.5	1.68	2.07
851.2	1.97	2.43
859.5	1.84	2.12
863.1	5.02	2.90
870.0	1.85	2.08
871.4	1.76	2.07
880.6	1.70	1.82
896.6	1.85	2.07
896.8	1.86	2.07
899.5	1.92	2.07
905.7	1.95	2.07
914.1	1.74	1.92
923.6	1.76	2.00
927.6	3.17	2.43
932.2	1.80	2.03
937.6	2.49	2.19
941.4	2.29	2.19
950.2	1.83	2.03
950.8	2.58	2.38
952.8	3.76	2.44
960.2	2.05	2.12
963.4	2.37	2.21
963.9	2.70	2.32
967.6	1.83	2.10
972.9	1.82	2.06
976.0	3.02	2.33
978.0	5.49	2.65
982.2	3.74	2.51
982.8	1.95	2.11
992.2	4.43	2.57
996.0	2.33	2.20
1000.7	4.08	2.57
1004.2	1.90	2.13
1009.8	4.08	2.55
1018.2	3.11	2.45
1020.4	1.78	2.08
1020.5	3.70	2.54
1021.0	2.78	2.34
1027.0	2.59	2.40
1028.8	1.78	2.03
1030.6	4.85	2.66
1045.4	2.01	2.16

1046.4	2.51	2.32
1050.0	3.22	2.46
1055.9	2.06	2.19
1063.6	4.15	2.59
1064.5	2.07	2.25
1072.8	1.97	2.15
1092.0	3.11	2.44
1100.9	3.64	2.47
1108.9	1.94	2.17
1111.4	3.31	2.47
1117.6	1.91	2.16
1120.5	3.74	2.53
1121.3	2.78	2.41
1125.8	3.18	2.48
1127.5	3.20	2.42
1129.6	2.04	2.17
1131.3	1.99	2.20
1132.1	2.23	2.23
1133.9	2.86	2.38
1139.4	4.18	2.54
1142.3	2.67	2.30
1145.2	2.04	2.21
1145.8	2.68	2.28
1150.2	3.82	2.45
1158.6	3.87	2.50
1161.6	3.07	2.33
1163.9	2.00	2.20
1166.4	2.70	2.31
1171.3	3.05	2.45
1173.9	2.06	2.19
1179.0	3.59	2.48
1182.0	2.87	2.25
1186.3	2.70	2.36
1188.7	4.38	2.54
1193.6	2.87	2.34
1196.3	3.26	2.43
1202.8	2.72	2.34
1205.5	3.20	2.44
1207.4	1.96	2.11
1212.3	3.08	2.38
1220.3	2.60	2.28
1229.2	2.80	2.31
1233.6	3.67	2.47
1237.6	2.52	2.32
1244.5	3.34	2.41
1247.4	2.67	2.31
1253.2	3.29	2.58
1261.7	3.22	2.34

1262.5	2.75	2.30
1266.1	3.14	2.43
1267.4	2.65	2.38
1268.3	2.70	2.38
1273.1	2.54	2.31
1277.3	2.80	2.32
1280.8	3.43	2.41
1286.2	3.77	2.47
1289.6	3.50	2.45
1295.3	3.68	2.49
1299.7	4.07	2.51
1304.2	3.34	2.41
1308.7	3.23	2.40
1313.1	3.02	2.33
1318.3	2.65	2.38
1322.4	3.41	2.42
1326.6	2.80	2.31
1331.3	3.97	2.53
1336.2	3.50	2.49
1340.1	3.94	2.51
1342.4	3.82	2.50
1344.5	3.52	2.49
1347.7	2.99	2.45
1350.2	3.59	2.52
1352.8	4.66	2.60
1353.6	2.79	2.41
1355.1	2.73	2.41
1358.6	3.70	2.54
1365.4	2.22	2.27
1372.1	4.58	2.63
1374.4	2.21	2.22
1380.9	3.81	2.55
1396.1	2.40	2.29
1401.9	2.88	2.46
1413.5	2.25	2.26
1425.5	2.25	2.29
1428.8	2.11	2.22
1429.4	4.94	2.68
1437.1	5.00	2.67
1441.5	2.68	2.41
1446.2	2.14	2.30
1447.1	5.19	2.68
1457.2	4.88	2.66
1464.3	4.13	2.58
1466.4	2.30	2.33
1469.1	2.82	2.44
1486.6	2.41	2.43
1495.6	2.66	2.37

1504.6	2.94	2.28
1505.2	4.05	2.61
1513.9	3.47	2.56
1523.0	2.45	2.36
1523.4	2.44	2.36
1549.6	2.39	2.37
1549.9	5.04	2.68
1559.4	4.31	2.59
1568.6	2.53	2.31
1572.6	2.30	2.23
1581.4	3.76	2.56
1590.3	3.18	2.51
1590.9	2.37	2.30
1596.1	3.21	2.53
1589.5	2.95	2.49
1603.8	3.42	2.54
1612.6	2.47	2.36
1616.7	3.27	2.54
1619.2	2.25	2.30
1623.2	2.35	2.28
1625.3	2.59	2.42
1631.6	2.36	2.39
1634.6	2.50	2.42
1640.2	5.14	2.71
1641.3	4.50	2.56
1645.0	5.41	2.79
1649.7	4.54	2.59
1654.0	5.87	2.82
1657.8	5.33	2.80
1662.3	5.46	2.82

DSDP SITE 391

<u>DEPTH</u>	<u>Vp</u>	<u>DENSITY</u>	<u>IMPEDANCE</u>	<u>POROSITY</u>
2.3	1.47	1.49		77.6
4.9	1.48	1.63		93.6
8.0	1.48	1.65	2.44	88.4
88.6	1.49	1.44	2.16	35.1
88.7	1.49			
92.1	1.49			
92.9	1.49			
93.6	1.52			
94.3	1.52	1.73	2.63	48.7
94.6	1.52			
149.1		1.79		53.7
152.1		1.94		48.0
204.4	1.70			
205.0	1.62	1.91	3.09	48.3
205.3	1.70			
207.8		1.91		50.9
260.2	1.72			
261.0	1.79			
261.7	1.71			
262.2		1.80		54.4
262.3	1.69			
263.3	1.70			
263.8	1.68			
265.0	1.78			
265.2		1.77		55.2
265.5	1.87			
266.7	1.85			
268.1	1.82			
268.3		1.84		51.4
316.8	1.81			
317.5	1.73			
317.6	1.75			
318.4	1.75	1.89	3.29	47.6
319.2	1.81			
320.0	1.83			
320.4	1.85			
321.7	2.24			
321.8	2.12	2.00	4.24	41.7
322.2	1.92			
323.6	2.03			
326.1	1.66			
326.8		1.53		64.7
330.9		1.55		63.9
332.4		1.47		64.0
336.4		1.48		67.3
355.3	1.79			
355.7	1.83			
356.9	1.77			
357.2		1.81		49.4

357.7	1.75			
358.4	1.78			
359.2	1.78			
360.0	1.85			
360.8	1.79			
361.8	1.81			
363.1		1.81		49.7
374.2	1.87			
375.4	1.87a			
376.1		1.84		48.8
376.4	1.85a			
377.0	1.85a			
379.1	1.87a	1.83	3.42	49.0
380.1	1.85a			
381.1	1.89			
381.5	1.86	1.85	3.44	48.3
413.1	1.91			
413.6	1.90			
414.4	1.94	1.84	3.57	48.3
414.6	1.94			
415.1	1.95			
416.3	1.92			
417.8	1.95			
418.2	1.98			
420.3	1.98			
420.8	1.92			
472.0	2.09			
474.6		1.93		43.3
477.1	2.36a			
526.1	1.65a			
526.2	1.77a			
527.6	1.91a	1.90	3.63	44.7
529.1	1.93a			
530.6	1.98a			
533.5	1.94a			
533.6	1.90a			
555.2	1.77a			
556.5	1.70a	1.57	2.67	63.3
569.9	1.94a			
570.7	1.98a	1.97	3.90	40.7
572.3	1.91a			
573.8	3.33a	2.29	7.63	22.1
574.3	1.75a			
585.4	2.01a		3.94	
585.5		1.96		40.9
587.0	1.91a			
587.4	1.91a			
588.3	1.93a			
640.8	1.69a			
642.2	1.75a			
643.6	1.69a	1.65	2.79	60.1
645.5	2.05a			
646.9	2.06a	2.03	4.18	38.4
650.0		1.62		38.0

653.0		2.00	42.7
656.0		1.95	43.5
669.4	1.87	1.96	
839.4	2.27	2.59	
841.2	2.20	1.99	
924.9	1.84	2.05	
927.9	2.31	2.06	
954.8	2.12	2.08	
1002.9	1.88	2.08	
1004.1	4.47		
1010.8	2.09	2.25	
1013.0	2.54	2.36	
1013.4	5.43		
1020.7	2.03		
1021.9	2.09	2.10	
1023.8	4.53		
1024.9	1.47	2.20	
1030.2	3.61		
1031.3	4.87		
1031.8	5.06		
1091.3	2.19		
1126.6	2.15	2.26	
1132.6	2.19	2.19	
1134.9	4.15	2.51	
1135.9	3.23		
1137.5	2.43	2.22	
1139.4	3.29		
1144.1	2.19		
1145.0	3.67		
1147.0	2.52		
1148.6	3.48	2.43	
1153.9	4.45		
1154.5	3.86	2.44	
1155.4	2.65		
1155.7	3.82		
1157.9	2.33	2.30	
1164.8	3.17	2.39	
1165.0	2.65		
1167.7	2.42	2.25	
1172.5	2.63		
1173.4	2.31		
1174.8	2.97	2.32	
1176.7	2.28		
1178.5	3.84		
1182.4	2.84		
1182.8	2.33		
1184.2	2.08		
1185.7	3.51		
1191.7	3.41		
1193.0	2.29	2.22	
1193.9	3.40	2.38	
1195.3	2.30	2.24	
1197.2	2.33		
1198.8	3.21	2.35	

Appendix A-2. Listing of Laboratory-measured Physical Properties for Sediments from DSDP Holes 417 and 418

DSDP SITE 417

<u>DEPTH</u>	<u>Vp</u>	<u>DENSITY</u>	<u>ACOUSTIC IMPEDANCE</u>	<u>POROSITY</u>	<u>SHEAR STRENGTH</u>
0.8		1.51		71.9	
1.1					0.06
3.1		1.45		67.1	
3.2					0.05
3.7	1.49		(2.29)2.26		0.08
3.8					
5.3		g1.54			
5.9		1.52			0.08
6.7					0.08
6.9		1.52			0.05
7.7					
9.4		1.59			0.08
9.6					
12.3	1.50	g1.59	(2.39)2.51		0.14
12.4					
12.6		1.67		78.6	
19.0					0.14
19.1		1.68			
19.3					0.09
21.5		1.68			
22.2					0.15
23.1	1.50				
23.4	1.50				
23.6	1.52				
23.7					0.14
23.9	1.51		(2.43)2.48		
24.8		g1.61			
24.3		1.64		75.2	
37.4		1.71		75.6	
37.5					0.26
38.7					0.23
39.1	1.50		2.55		
46.8					0.15
47.0		1.70			
49.7					0.27
49.8	1.49		(2.29)2.46		
50.0		1.67		74.2	
50.7					0.14
51.7		1.69			0.19
53.8					0.13
54.0		1.51		78.9	
54.4		g1.54			
55.6					0.16
66.4		1.62		60.0	0.28
68.1					0.16
69.0		1.67			
69.1					0.25
69.4		g1.59			

69.6	1.51	(2.40)2.52	
71.6			0.50
75.2			0.40
75.7	1.66		
76.9			0.56
78.3			0.26
78.4	1.73		71.3
78.8	1.52	(2.46)2.63	
80.2	g1.62		
80.5			0.33
81.2	1.65		75.3
81.3			0.26
84.8			0.31
86.7	g1.66		
86.9			0.53
87.6			0.70
87.9	1.62		
88.0	1.54	(2.56)2.49	
89.3			0.64
94.4	1.91		73.3
95.8			0.65
97.2			0.80
97.8	1.82		71.4
99.2	g1.68		
99.3	1.54	(2.59)2.80	
99.9			0.92
100.0	1.84		
100.7	1.53		70.8
104.5	1.75		72.0
107.4	1.54	(2.56)2.70	
109.0	g1.66		
116.4	1.71		
117.9	1.57	(2.43)2.68	
119.7	1.55		85.7
119.8	g1.55		
124.6	1.75		69.9
126.2	1.58	(2.53)2.50	
129.2	g1.60		
129.3	1.58		69.4
132.1	1.67		
133.6	1.54	(2.60)2.57	
134.7	1.54		
135.3	1.64		
135.8	g1.69		
145.1	1.75		
148.2	1.75		71.1
149.8	1.61	(2.72)2.82	
150.5	1.74		
150.7	g1.69		
163.0	1.73		72.8
163.6	1.83		
163.7	1.55		
164.2	g1.57		
173.2	1.57		49.9

173.5	1.59		(2.64)2.50	
175.3		g1.66		
179.7		1.78		62.5
181.4	1.54		(2.53)2.74	
185.2		1.75		65.2
185.3		g1.64		
189.6		1.78		69.1
190.8		g1.64		
191.0	1.62		(2.66)2.84	
192.0		1.75		
192.1		1.71		70.9
204.2	1.60	1.71	2.74	59.0
212.1	1.66			
221.1	1.61		2.53	
221.3		1.57		52.1
230.8		1.8		50.
231.9	1.62		2.85	
233.5		1.63		
239.9	1.73	1.66	2.87	59.5
250.1		1.40		
252.7		1.76		54.1
253.3	1.63			
258.9		1.90		52.8
259.0	1.66		3.15	
267.9		1.76		
268.8		1.73		52.2
271.6		1.76		
272.5		1.80		53.0
273.3	1.65		2.97	
274.8		1.66		48.7
278.5		1.90		65.5
278.7	1.61		3.06	
279.1	2.04	1.77	3.61	53.9
287.5		1.66		
297.8	1.66	1.71	2.84	59.5
306.6	1.73	1.64	2.84	55.9
315.8	2.05	1.99	4.08	57.0
327.6	2.25	2.12	4.77	38.8
336.8	1.85	1.97	3.64	48.8
345.4	5.38	2.80	15.1	7.7
352.6	5.40	2.83	15.3	6.2
358.3	5.25	2.77	14.5	9.4
362.7	5.46	2.80	15.3	7.3
367.7	5.56	2.83	15.7	6.4
371.4	5.16	2.77	14.3	10.1
377.6	5.41	2.79	15.1	7.5
382.8	5.35	2.80	15.0	7.9
384.8	5.52	2.81	15.1	6.1
385.6	5.02	2.72	13.7	10.1
390.6	5.20	2.72	14.1	9.4
395.0	5.67	2.86	16.2	4.7
395.3	5.07	2.68	13.6	8.8
397.6	5.18	2.75	14.2	8.8
400.1	4.56	2.52	11.5	13.2

414.2	5.04	2.76	13.9	8.3
419.2	5.79	2.90	16.8	3.0
424.0	5.65	2.86	16.2	3.6
427.1	5.67	2.87	16.3	3.3
431.5	5.87	2.89	17.0	2.7
437.4	5.66	2.83	16.0	4.6
439.7	5.31	2.77	14.7	7.2
445.2	5.67	2.85	16.2	4.1
446.6	5.64	2.84	16.0	4.8
450.7	5.58	2.84	15.8	5.0
453.3	5.51	2.80	15.4	6.0
457.2	5.50	2.79	15.3	4.8
461.0	5.79	2.67	15.5	3.5
463.6	5.71	2.89	16.5	3.5
464.7	3.83			
466.0	3.67	2.38	8.7	
467.0	5.85	2.86	16.7	3.4
471.8	5.46	2.77	15.1	9.5
477.3	5.80	2.82	16.4	8.0
482.5	5.97	2.74	16.4	5.5
487.5	5.30	2.72	14.4	11.6
492.0	5.56	2.84	15.8	8.4
496.4	5.61	2.84	15.9	7.0
499.7	5.72	2.89	16.5	6.5

DSDP SITE 418

<u>DEPTH</u>	<u>V_p</u>	<u>DENSITY</u>	<u>ACOUSTIC IMPEDANCE</u>	<u>POROSITY</u>
7.3	1.65	1.24	2.05	85.7
18.1		1.55		
18.3	1.48		2.28	
27.6		1.54		69.2
29.1	1.49			
29.9	1.47		2.34	
30.3		1.59		
31.3	1.52			
31.6	1.49			
37.1	1.55	1.59	2.46	68.4
37.8	1.48			
46.4		1.41		73.2
46.7	1.61		2.27	
47.4	1.59			
49.4		1.57		65.6
60.6	1.46	1.58	2.31	71.5
61.0	1.50			
61.5	1.49			
68.6	1.47	1.60	2.35	69.9
68.8	1.51			
69.6	1.49			
75.0		1.88		62.5
75.6	1.57		2.95	
79.5	1.53	1.54	2.39	78.3
79.7	1.54			
80.2	1.52			
82.5		1.40		
84.4	1.47	1.46	2.12	74.5
85.2	1.50			
93.8	1.47	1.57	2.31	71.1
94.1	1.51			
94.5	1.50			
94.8	1.54			
95.0	1.52			
96.7	1.50		2.18	
97.2		1.45		
103.3	1.58			
104.0	1.56		2.20	
106.8		1.41		61.9
111.2	1.62	1.63	2.64	68.7
111.7	1.54			
115.3		1.51		
121.5	1.54		2.53	
131.3	1.44	1.77	2.55	85.4
132.4	1.55			
139.3	1.47	1.66	2.44	62.8
141.6	1.45			
150.6		1.64		75.8
158.8	1.56			
159.3	1.61		2.66	
168.1	1.41		2.14	
168.2		1.52		

168.8	1.52			
172.7		1.59		63.7
172.8	1.61		2.56	
177.7		1.67		
187.2		1.61		
187.3	1.52		2.45	
187.8	1.45			
196.6	1.66			
197.5	1.67			
197.9	1.70			
198.6	1.70		2.77	
198.8		1.63		
205.9	1.78			
206.1	1.74		2.23	
206.8		1.28		
215.3	1.70			
215.8		1.63		
215.9	1.67		2.72	
225.0	1.69			
225.7	1.71		2.91	
227.2		1.70		
235.0	1.71			
235.5	1.66			
235.8	4.75			
244.0	1.72			
244.4		1.87		
244.5	1.68		3.14	
244.9	1.65			
245.3	5.19	2.55	13.23	
253.6	1.52			
254.2	1.63			
255.6		1.68		
256.8	1.62		2.72	
263.6	1.56			
301.7	1.62			
303.1	1.62	1.82	2.95	52.8
321.8	5.00	2.65	13.3	12.0
323.4	5.71	2.84	16.2	5.3
330.0	4.97	2.70	13.4	9.5
332.0	4.86	2.62	12.7	11.7
333.0	5.21	2.69	14.0	10.3
335.3	4.93	2.65	13.1	11.3
337.1	5.09	2.70	13.7	9.4
340.0	5.89	2.86	16.9	3.7
342.5	5.93	2.86	17.0	6.7
346.1	3.98	2.44	9.7	23.5
349.0	5.70	2.85	16.3	4.9
351.8	6.17	2.89	17.8	2.8
354.0	6.26	2.93	18.3	2.0
357.6	6.11	2.91	17.8	2.5
360.2	5.95	2.91	17.3	2.3
367.4	5.59	2.79	15.6	6.8
376.5	5.95	2.86	17.0	4.8

383.0	5.63	2.80	15.8	5.8
385.1	5.88	2.87	16.9	4.3
387.7	5.22	2.71	14.2	8.0
393.7	5.30	2.73	14.5	8.8
395.9	5.31	2.71	14.4	8.1
403.2	3.47	2.29	8.0	30.1
405.8	5.13	2.66	13.7	8.6
416.5	5.72	2.83	16.2	4.5
419.2	5.38	2.72	14.6	6.2
423.2	5.49	2.75	15.1	6.9
425.1	3.44	2.30	7.9	30.2
441.4	4.54	2.50	11.4	16.9
443.6	5.38	2.74	14.7	6.0
447.5	5.66	2.82	16.0	5.7
449.3	5.64	2.82	15.9	5.1
455.1	4.14	2.39	9.9	22.9
458.3	5.10	2.67	13.6	9.7
461.3	5.21	2.72	14.2	7.2
464.2	4.54	2.54	11.5	13.8
467.8	5.29	2.73	14.4	7.3
470.7	5.66	2.82	16.0	4.8
476.8	4.57	2.56	11.7	11.6
479.9	4.95	2.65	13.1	8.7
482.9	5.42	2.77	15.0	6.7
486.0	5.24	2.70	14.2	7.3
489.9	5.67	2.82	16.0	5.2
497.8	5.13	2.74		
499.5	5.57	2.77	15.4	5.9

Appendix A-3. Listing of Laboratory-measured Physical Properties for Sediments from DSDP Site 386

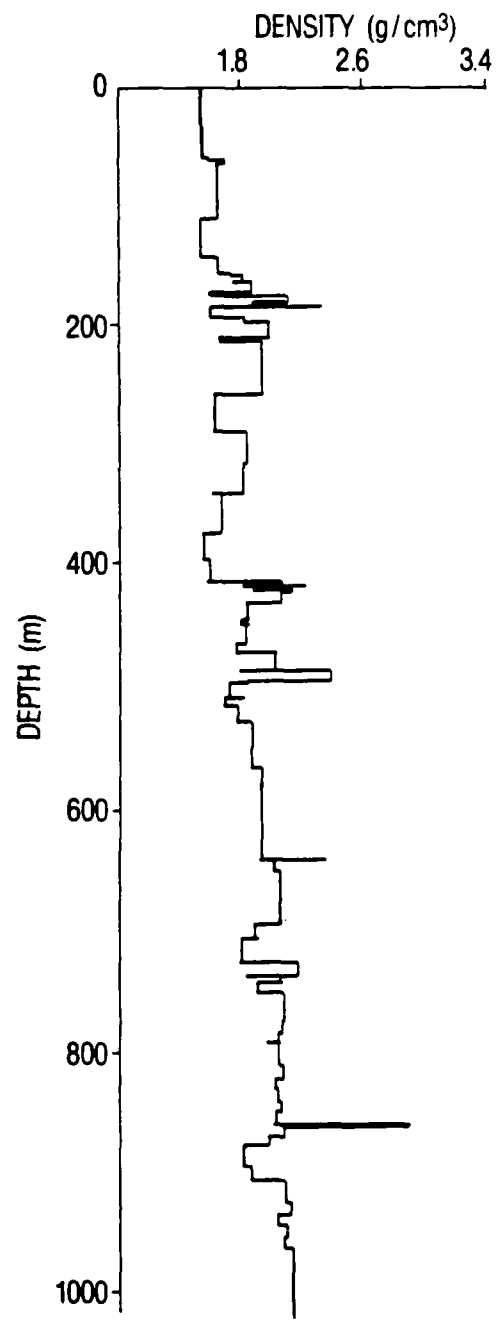
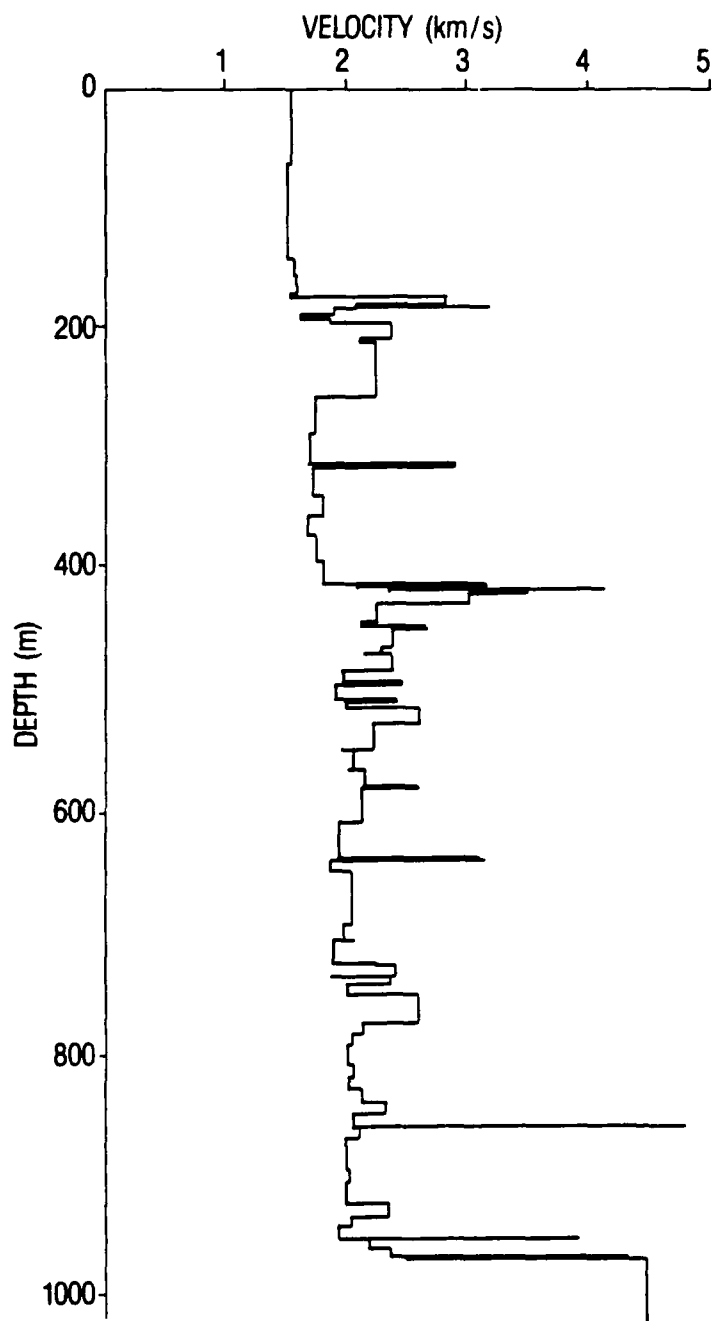
DSDP SITE 386

<u>DEPTH</u>	<u>Vp</u>	<u>DENSITY</u>	<u>POROSITY</u>	<u>Vs</u>
54.7	0.00	1.54	69.00	0.0000
55.4	0.00	1.55	68.00	0.0000
55.9	0.00	1.57	66.00	0.0000
56.9	0.00	1.53	68.00	0.0000
57.5	0.00	1.59	66.00	0.0000
58.3	0.00	1.59	65.00	0.0000
58.8	0.00	1.63	67.00	0.0000
59.6	1.54	1.70	57.00	0.2244
60.0	0.00	1.64	68.00	0.0000
61.4	1.50	0.00	0.00	0.3445
107.5	1.50	1.52	68.00	0.3445
139.4	1.56	1.65	66.00	0.2887
152.6	0.00	0.00	0.00	0.0000
152.8	1.59	1.74	53.00	0.3228
153.4	0.00	0.00	0.00	0.0000
154.2	0.00	0.00	0.00	0.0000
155.0	0.00	1.81	53.00	0.0000
155.2	1.58	0.00	0.00	0.3115
158.6	0.00	0.00	0.00	0.0000
159.5	0.00	0.00	0.00	0.0000
160.1	1.57	1.73	56.00	0.3001
160.3	0.00	0.00	0.00	0.0000
161.5	1.59	1.87	60.00	0.3228
169.4	1.53	1.59	62.00	0.1855
171.2	1.90	1.72	63.00	0.5293
171.6	2.72	2.11	44.00	1.1596
171.9	2.82	2.12	43.00	1.2376
177.7	2.06	1.87	57.00	0.6453
179.9	3.19	2.34	36.00	1.5262
180.2	1.89	1.60	70.00	0.5228
186.6	1.61	1.60	69.00	0.3456
187.2	0.00	0.00	0.00	0.0000
187.5	0.00	0.00	0.00	0.0000
189.4	1.85	1.81	59.00	0.4980
192.8	2.37	1.98	52.00	0.8866
206.3	2.10	1.65	66.00	0.6781
208.4	2.24	1.94	53.00	0.7852
253.8	1.75	1.62	67.00	0.4424
254.7	1.73	0.00	0.00	0.4324
289.3	1.78	1.62	66.00	0.4581
284.4	1.67	1.83	67.00	0.4047
310.9	2.90	0.00	0.00	1.3000
311.7	1.80	1.81	55.00	0.4690

311.7	1.71	0.00	0.00	0.4228
335.4	1.76	1.60	60.00	0.4475
335.8	1.79	1.67	66.00	0.4635
353.7	1.77	1.67	66.00	0.4527
353.7	1.66	0.00	0.00	0.4004
369.3	1.75	1.53	59.00	0.4424
370.1	1.73	1.54	61.00	0.4324
390.7	1.70	1.59	57.00	0.4181
390.8	1.80	1.58	62.00	0.4690
409.3	3.13	2.07	15.00	1.4794
410.1	2.06	1.80	24.00	0.6453
412.0	4.13	2.24	6.00	2.2594
412.2	2.34	1.86	41.00	0.8632
415.2	3.48	2.14	17.00	1.7524
416.3	3.00	2.06	33.00	1.3780
425.1	2.23	1.84	25.00	0.7774
440.4	2.09	1.79	46.00	0.6698
443.3	2.65	1.85	42.00	1.1050
443.5	2.36	1.82	44.00	0.8788
460.1	2.27	1.74	49.00	0.8086
466.2	2.12	1.78	47.00	0.6950
466.7	2.36	2.03	35.00	0.8738
482.2	2.14	1.76	48.00	0.7124
482.3	1.94	2.39	17.00	0.5561
490.4	2.45	1.83	41.00	0.9490
491.7	1.90	1.71	56.00	0.5293
505.0	2.40	1.83	51.00	0.9100
505.3	1.97	1.68	42.00	0.5771
511.1	2.12	1.70	45.00	0.6950
511.3	2.58	1.78	42.00	1.0504
524.1	2.20	1.87	43.00	0.7540
545.8	1.94	1.69	54.00	0.5561
546.7	2.05	1.86	43.00	0.6374
563.0	1.99	1.84	48.00	0.5916
563.2	2.14	1.93	41.00	0.7124
576.8	2.58	1.89	41.00	1.0504
577.5	2.10	1.92	44.00	0.6781
606.3	1.91	1.92	49.00	0.5358
638.9	3.13	2.36	23.00	1.4794
639.2	1.84	2.01	43.00	0.4920
647.4	2.05	2.04	43.00	0.6374
691.1	2.04	1.97	53.00	0.6295
691.2	1.95	1.88	54.00	0.5630
704.0	2.07	1.92	45.00	0.6534
704.1	1.87	1.73	47.00	0.5102
723.8	2.24	2.06	41.00	0.7852
724.5	2.37	2.17	37.00	0.8866
734.0	1.85	1.81	43.00	0.4980

734.4	2.36	2.06	40.00	0.8788
740.2	1.98	1.89	34.00	0.5843
749.4	2.14	2.02	39.00	0.7124
749.7	2.58	2.07	36.00	1.0504
772.4	2.10	2.05	39.00	0.6781
781.7	2.04	2.03	40.00	0.6295
781.9	2.02	2.04	43.00	0.6141
790.2	1.99	1.95	57.00	0.5916
791.3	1.98	2.03	39.00	0.5843
808.2	2.04	2.06	39.00	0.6295
819.3	1.99	2.06	39.00	0.5916
819.7	2.00	2.01	40.00	0.5990
828.6	2.10	2.03	41.00	0.6781
839.2	2.30	2.05	40.00	0.8320
846.4	2.02	2.02	40.00	0.6141
853.6	4.78	2.91	18.00	2.7664
859.0	2.08	2.07	40.00	0.6615
866.6	2.08	2.04	41.00	0.6615
866.7	1.95	1.96	44.00	0.5630
873.9	1.98	1.80	19.00	0.5843
893.5	2.00	1.84	41.00	0.5990
904.0	1.97	2.08	39.00	0.5771
922.1	2.33	2.12	36.00	0.8554
931.9	2.01	2.02	40.00	0.6065
941.0	1.90	2.09	39.00	0.5293
950.6	3.92	0.00	5.00	2.0956
950.7	2.16	2.06	40.00	0.7228
958.8	2.35	2.12	40.00	0.8710
965.3	4.17	0.00	0.00	2.2906
965.8	4.29	0.00	0.00	2.3842
966.3	2.45	0.00	0.00	0.9490
966.6	3.92	0.00	0.00	2.0956
966.8	4.45	0.00	0.00	2.5090

Appendix A-4. Plot of Laboratory-measured Velocity as a Function of Depth for Cores from Hole 386



Distribution List

002 A1 FCTS ASN (RE&S)
Department of the Navy
Asst Secretary of the Navy
(Research Engineering & System)
Washington DC 20350-1000

004 A3 FCTS CNO
Department of the Navy
Chief of Naval Operations
Attn: OP-951
Washington DC 20350-2000

FCNC
Director
National Oceanic Data Center
WSC1 Room 103
6001 Executive Blvd.
Attn: G. W. Withee
Rockville MD 20852

004 A3 FCTS CNO
Department of the Navy
Chief of Naval Operations
Attn: OP-987
Washington DC 20350-2000

005 A3 FCTS CNO
Department of the Navy
Oceanographer of the Navy
Attn: OP-096
Washington DC 20350

006 1303 500 E3D2 FCTS NAVAIRDEVCE
Commander
Naval Air Development Center
Warminster PA 18974-5000

007 1461 900 FKA1A FCTS COMNAVAIRSYSCOM
Commander
Naval Air Systems Command Headquarters
Washington DC 20361-0001

009 2130 600 E3D3 FCTS NAVCOASTSYSCEN
Commanding Officer
Naval Coastal Systems Center
Panama City FL 32407-5000

023 2925 905 FKA1B FCTS COMSPANAVWARSYSCOM
Commanding Officer
Space & Naval Warfare Sys Com
Washington DC 20363-5100

030 2980 500 E3D11 FCS NAVENVPRESRSCHFAC
Commanding Officer
Naval Environmental Prediction Research Facility
Monterey CA 93943-5006

031 3075 910 FKA1C FCTS COMNAVAFACENGCOM
Commander
Naval Facilities Eng Command Headquarters
200 Stovall St.
Alexandria VA 22332-2300

045 4488 200 E3C FCTS NORDA
Commanding Officer
Naval Ocean R&D Activity
Attn: Code 113
Stennis Space Center MS 39529-5004

045 4488 200 E3C FCTS NORDA
Commanding Officer
Naval Ocean R&D Activity
Attn: Code 125L (13)
Stennis Space Center MS 39529-5004

045 4488 200 E3C FCTS NORDA
Commanding Officer
Naval Ocean R&D Activity
Attn: Code 125P (1)
Stennis Space Center MS 39529-5004

045 4488 200 E3C FCTS NORDA
Commanding Officer
Naval Ocean R&D Activity
Attn: Code 105
Stennis Space Center MS 39529-5004

045 4488 200 E3C FCTS NORDA
Commanding Officer
Naval Ocean R&D Activity
Attn: Code 115
Stennis Space Center MS 39529-5004

045 4488 200 E3C FCTS NORDA
Commanding Officer
Naval Ocean R&D Activity
Attn: Code 200
Stennis Space Center MS 39529-5004

045 4488 200 E3C FCTS NORDA
Commanding Officer
Naval Ocean R&D Activity
Attn: Code 300
Stennis Space Center MS 39529-5004

047 3860 930 E3A FCS NRL
Commanding Officer
Naval Research Laboratory
Washington DC 20375

053 4480 100 FD1 FCS MCAFA/OCEANAV
Commander
Naval Oceanography Command
Stennis Space Center MS 39529-5000

059 4483 270 FD3 FCTS FLENUMOCEANEN
Commanding Officer
Fleet Numerical Ocean Center
Monterey CA 93943-5005

062 4485 365 FD2 MCAFA/NAVOCEANO
Commanding Officer
Naval Oceanographic Office
Stennis Space Center MS 39522-5001

065 4489 800 E3D4 FCTS NAVOCEANSYSCOM
Commander
Naval Ocean Systems Center
San Diego CA 92152-5000

068 5580 350 E3B FCS ONRBRO REG
Commanding Officer
ONR Branch Office
Box 39
FPO New York 09510-0700

069 5580 540 C20A FCS ONRWEST
Officer in Charge
Office of Naval Research Detachment, Pasadena
1030 E. Green Street
Pasadena CA 91106-2485

071 5856 E3D6 FCTS DTNSRDC
Commander
DW Taylor Naval Research Center
Bethesda MD 20084-5000

074 6214 950 E3D7 FCTS NAVSWC
Commander
Naval Surface Warfare Center
Dahlgren VA 22448-5000

076 6541 500 FCTS E3D9 NUSC
Commanding Officer
Naval Underwater Systems Center
Newport RI 02841-5047

085 7685 435 FT73 FCTS NAVPGSCOL
Superintendent
Naval Postgraduate School
Monterey CA 93943

098 5520 750 C4L FCS ONL
Director
Office of Naval Laboratories
Rm 866 Crystal Plaza Five
Washington DC 20360

131 C20J FCTS NUSCDET
Officer in Charge
Naval Underwater Sys Cen Det
New London CT 06320

136 B2A FCS DTIC
Defense Technical Info Cen
Attn: DTIC-DDAC (12)
Cameron Station
Alexandria VA 22314

298 A2A FCTS ONR
Director
Office of Naval Research
Attn: Code 10
800 N. Quincy St.
Arlington VA 22217-5000

800 WHOI FCS CONT REG
Director
Woods Hole Oceanographic Inst
86-96 Water St.
Woods Hole MA 02543

804 SCRIPPS FCS CONT REG
Director
University of California
Scripps Institute of Oceanography
PO Box 6049
San Diego CA 92106

376 C20I FCTS NAVSURWPNCEN
Officer in Charge
White Oak Laboratory
Naval Surface Warfare Center Det
10901 New Hampshire Ave.
Attn: Library
Silver Spring MD 20903-5000

034 3135 550 FT46 FCTS
Commanding Officer
Fleet Anti-Sub Warfare Training
Center Atlantic
Naval Station
Norfolk VA 23511-6495

Brooke Farquhar
NORDA Liaison Office
Room 802 Crystal Plaza #5
2211 Jeff Davis Hwy.
Arlington VA 22202-5000

UNCLASSIFIED

SECURITY CLASSIFICATION OF THIS PAGE

REPORT DOCUMENTATION PAGE				
1a. REPORT SECURITY CLASSIFICATION Unclassified		1b. RESTRICTIVE MARKINGS None		
2a. SECURITY CLASSIFICATION AUTHORITY		3. DISTRIBUTION/AVAILABILITY OF REPORT Approved for public release; distribution is unlimited.		
2b. DECLASSIFICATION/DOWNGRADING SCHEDULE				
4. PERFORMING ORGANIZATION REPORT NUMBER(S) NORDA Report 199		5. MONITORING ORGANIZATION REPORT NUMBER(S) NORDA Report 199		
6. NAME OF PERFORMING ORGANIZATION Naval Ocean Research and Development Activity		7a. NAME OF MONITORING ORGANIZATION Naval Ocean Research and Development Activity		
6c. ADDRESS (City, State, and ZIP Code) Ocean Acoustics and Technology Directorate Stennis Space Center, Mississippi 39529-5004		7b. ADDRESS (City, State, and ZIP Code) Ocean Acoustics and Technology Directorate Stennis Space Center, Mississippi 39529-5004		
8a. NAME OF FUNDING/SPONSORING ORGANIZATION Naval Ocean Research and Development Activity	8b. OFFICE SYMBOL (If applicable) 200	9. PROCUREMENT INSTRUMENT IDENTIFICATION NUMBER		
8c. ADDRESS (City, State, and ZIP Code) Ocean Acoustics and Technology Directorate Stennis Space Center, Mississippi 39529-5004		10. SOURCE OF FUNDING NOS		
		PROGRAM ELEMENT NO. 62435N	PROJECT NO. 00101	TASK NO. 100
		WORK UNIT NO. DN255056		
11. TITLE (Include Security Classification) Geologic Study of Five Sites in the Western North Atlantic Ocean				
12. PERSONAL AUTHOR(S) M. S. Grim, F. A. Bowles, J. F. Gettrust, and D. A. Burns				
13a. TYPE OF REPORT Final	13b. TIME COVERED From _____ To _____	14. DATE OF REPORT (Yr., Mo., Day) February 1989		15. PAGE COUNT 56
16. SUPPLEMENTARY NOTATION				
17. COSATI CODES			18. SUBJECT TERMS (Continue on reverse if necessary and identify by block number) ULF/VLF, LSAP, borehole seismology, shear compressional propagation modeling	
FIELD	GROUP	SUB. GR.		
19. ABSTRACT (Continue on reverse if necessary and identify by block number) For an accurate geoacoustic model to be constructed the geology of the area must be well understood. In some areas modeling may not be successful because small-scale lithologic and topographic changes are not recognized from the available data. Currently, we do not have the ability to obtain complete measurements of such sediment properties as velocity and density from a drill hole. Laboratory and in situ measurements do not agree, and attempts to reconcile the two have not been completely effective. In constructing our geoacoustic models we have tried to build on the work of others. In our models, we have added high-velocity stringers which are almost always present in nature; for example, worldwide occurrences of chert have been documented by Deep-Sea Drilling Project (DSDP) cores. We chose five areas of the western North Atlantic Ocean and constructed geoacoustic models for each area. For two areas we used the laboratory and seismic data collected during DSDP studies, as well as published reports, to construct detailed models. For the remaining three areas we have tabulated generalized sediment velocity and lithology information from published reports. In working on data from these five sites it became apparent to us that some areas (for example, the Bahama Banks) have such rugged topography and such variable lithology that traditional modeling attempts probably will be unsuccessful unless the geology is known in great detail. Some continental margin shallow-water sites and some deep ocean sites, such as DSDP site 417/418, are much more predictable and should be easier to model; however, even site 417/418 has unique geologic factors that will cause actual seismic propagation to differ from our model predictions. However, deviations from predicted values should be reasonably small at low (5-50 Hz) frequencies.				
20. DISTRIBUTION/AVAILABILITY OF ABSTRACT UNCLASSIFIED/UNLIMITED <input type="checkbox"/> SAME AS RPT. <input checked="" type="checkbox"/> DTIC USERS <input type="checkbox"/>		21. ABSTRACT SECURITY CLASSIFICATION Unclassified		
22a. NAME OF RESPONSIBLE INDIVIDUAL F. A. Bowles		22b. TELEPHONE NUMBER (Include Area Code) (601) 688-5464		22c. OFFICE SYMBOL Code 361